human leukaemic T cells. Nature. 1981;294:770-771.

37. Yamamoto N, Okada M, Koyanagi Y, Kannagi M, Hinuma Y. Transformation of human leukocytes by cocultivation with an adult T cell leukemia virus producer cell line. Science. 1982;217:737-739.

38. Popovic M, Sarin PS, Robert-Gurroff M, et al. Isolation and transmission of human retrovirus (human T-cell leukemia virus). Science. 1983;219:856-859.

39. Koeffler HP, Chen IS, Golde DW. Characterization of a novel HTLV-infected cell line. Blood. 1984;64:482-490.

40. Miyoshi I, Kubonishi I, Sumida M, et al. A novel T-cell line derived from adult T-cell leukemia. Gann. 1980;71:155-156.

41. Maeda M, Shimizu A, Ikuta K, et al. Origin of human T-lymphotrophic virus I-positive T cell lines in adult T cell leukemia. Analysis of T cell receptor gene rearrangement. J Exp Med. 1985;162:2169-2174.

42. Ishiyama M, Shiga M, Sasamoto K, Mizoguchi M, He P. A new sulfonated tetrazolium salt that produces a highly water-soluble formazan dye. Chem Pharm Bull. 1993;41:1118-1122.

43. Zhang C, Ao Z, Seth A, Schlossman SF. A mitochondrial membrane protein defined by a novel monoclonal antibody is preferentially detected in apoptotic cells. J Immunol. 1996;157:3980-3987.

44. Seth A, Zhang C, Letvin NL, Schlossman SF. Detection of apoptotic cells from peripheral blood of HIV-infected individuals using a novel monoclonal antibody. AIDS. 1997;11:1059-1061.

45. Matsumoto K, Shibata H, Fujisawa J, et al. Human T-cell leukemia virus type 1 Tax protein transforms rat fibroblasts via two distinct pathways. J Virol. 1997;71:4445-4451.

46. Dewan MZ, Watanabe M, Terashima K, et al. Prompt tumor formation and maintenance of constitutive NF-κB activity of multiple myeloma cells in NOD/SCID/γc^{null} mice. Cancer Sci. 2004;95:1-5.

47. Duyao MP, Kessler DJ, Spicer DB, et al. Transactivation of the c-myc promoter by human T cell leukemia virus type 1 tax is mediated by NFκB. J Biol Chem. 1992;267:16288-16291.

48. Huang Y, Ohtani K, Iwanaga R, Matsumura Y, Nakamura M. Direct trans-activation of the human cyclin D2 gene by the oncogene product Tax of human T-cell leukemia virus type I. Oncogene. 2001;20:1094-1102.

49. Mitsiades N, Mitsiades CS, Poulaki V, et al. Biologic sequelae of nuclear factor-κB blockade in multiple myeloma: therapeutic applications. Blood. 2002;99:4079-4086.

50. Mori N, Fujii M, Cheng G, et al. Human T-cell leukemia virus type I tax protein induces the expression of anti-apoptotic gene Bcl-x_L in human T-cells through nuclear factor-κB and c-AMP responsive element binding protein pathways. Virus Genes. 2001;22:279-287.

51. Nicot C, Mahieux R, Takemoto S, Franchini G. Bcl-X_L is up-regulated by HTLV-I and HTLV-II in vitro and in ex vivo ATLL samples. Blood. 2000;96:275-281.

52. Tamura K. Clinical classification of adult T-cell leukemia and its complications. Rinsho Byori. 1996;44:19-23.

53. Watanabe T. HTLV-1-associated diseases. Int J Hematol. 1997;66:257-278.

54. Imada K, Takaori-Kondo A, Sawada H, et al. Serial transplantation of adult T cell leukemia cells into severe combined immunodeficient mice. Jpn J Cancer Res. 1996;87:887-892.

55. Kondo A, Imada K, Hattori T, et al. A model of in vivo cell proliferation of adult T-cell leukemia. Blood. 1993;82:2501-2509.

56. Phillips KE, Herring B, Wilson LA, et al. IL-2Rα-directed monoclonal antibodies provide effective therapy in a murine model of adult T-cell leukemia by a mechanism other than blockade of IL-2/IL-2Rα interaction. Cancer Res. 2000;60:6977-6984.

57. Chu ZL, McKinsey TA, Liu L, Gentry JJ, Malim MH, Ballard DW. Suppression of tumor necrosis factor-induced cell death by inhibitor of apoptosis c-IAP2 is under NF-κB control. Proc Natl Acad Sci U S A. 1997;94:10057-10062.

58. Norvir, ritonavir product monograph. North Chicago, IL: Abbott Laboratories, 1997.

59. Gatti G, Di Biagio A, Casazza R, et al. The relationship between ritonavir plasma levels and side-effects: implications for therapeutic drug monitoring. AIDS. 1999;13:2083-2089.

Clonal analysis of thymus-repopulating cells presents direct evidence for self-renewal division of human hematopoietic stem cells

Takashi Yahata, Shizu Yumino, Yin Seng, Hiroko Miyatake, Tomoko Uno, Yukari Muguruma, Mamoru Ito, Hiroyuki Miyoshi, Shunichi Kato, Tomomitsu Hotta, and Kiyoshi Ando

To elucidate the in vivo kinetics of human hematopoietic stem cells (HSCs), $CD34^+CD38^-$ cells were infected with lentivirus vector and transplanted into immunodeficient mice. We analyzed the multilineage differentiation and self-renewal abilities of individual thymus-repopulating clones in primary recipients, and their descending clones in paired secondary recipients, by tracing lentivirus gene integration sites in each lymphomyeloid progeny using a linear amplification-mediated polymerase chain reaction (PCR) strategy. Our clonal analysis revealed that a single human thymus-repopulating cell had the ability to produce lymphoid and myeloid lineage cells in the primary recipient and each secondary recipient, indicating that individual human HSCs expand clonally by self-renewal division. Furthermore, we found that the proportion of HSC clones present in the $CD34^+$ cell population decreased as HSCs replicated during extensive repopulation and also as the differentiation capacity of the HSC clones became limited. This indicates the restriction of the ability of individual HSCs despite the expansion of total HSC population. We also demonstrated that the extensive self-renewal potential was confined in the relatively small proportion of HSC clones. We conclude that our clonal tracking studies clearly demonstrated that heterogeneity in the self-renewal capacity of HSC clones underlies the differences in clonal longevity in the $CD34^+$ stem cell pool. (Blood. 2006;108:2446-2454)

Introduction

Self-renewal and multilineage differentiation are the 2 fundamental abilities that define hematopoietic stem cells (HSCs) and distinguish them from progenitors. Severe combined immunodeficient mouse (SCID)–repopulating cells (SRCs), originally identified by their ability to reconstitute hematopoiesis in nonobese diabetic (NOD)/SCID mice, are thought to represent human HSCs that are useful clinically to repopulate human recipients.[1-3] Unlike murine HSCs that have been purified and analyzed at the single-cell level,[4] viral gene-marking is the only strategy for the in vivo clonal analysis of human HSCs.[5] Using this approach, several studies documented heterogeneity among SRC clones and implied that some clones have the ability to differentiate into B-lymphoid and myeloid lineages and to self-renew.[6-12] A major shortcoming of using the NOD/SCID mouse model is a lack of reproducible human T-lymphocyte repopulation. Consequently, the multilineage differentiation capacity of SRCs in NOD/SCID recipients has been assessed by reconstitution of only B-lymphoid and myeloid lineages. Because a close relationship between B-lymphocyte and macrophage differentiation has been indicated,[13,14] current analyses cannot clearly distinguish true HSCs from lineage-restricted progenitors such as B-lymphocyte/macrophage progenitors. As a result, the multilineage differentiation and self-renewal of HSCs represented by a single SRC are yet to be proven.

Along with other investigators, we demonstrated that phenotypically normal and polyclonal human T lymphocytes were reproducibly repopulated from human cord blood $CD34^+$ cells in the NOD/SCID/common γ chain (cγ)–null (NOG) mouse.[15-17] Having this unique environment that permits human thymopoiesis, the NOG recipient serves as an excellent model to study self-renewal, as well as multilineage differentiation, of human HSCs. HSCs can be identified as thymus-repopulating cells and distinguished from short-lived oligopotent or monopotent progenitors. Thymopoiesis requires constant recruitment of progenitors into the thymus, which eventually produces mature T lymphocytes in a relatively short period of time.[18,19] Therefore, to maintain thymopoiesis in recipient mice, transplanted HSCs must divide without loss of thymus-repopulating activity. Several classes of SRCs that differ in their proliferative and self-renewal potential have been reported.[20-22]

From the Division of Hematopoiesis, Research Center for Regenerative Medicine, Tokai University School of Medicine, Isehara, Kanagawa; the Department of Hematology, Tokai University School of Medicine, Isehara, Kanagawa; the Central Institute for Experimental Animals, Kawasaki, Kanagawa; the BioResource Center, RIKEN Tsukuba Institute, Tsukuba, Ibaraki; and the Department of Cell Transplantation & Regenerative Medicine, Tokai University School of Medicine, Isehara, Kanagawa, Japan.

Submitted February 8, 2006; accepted May 20, 2006. Prepublished online as *Blood* First Edition Paper, June 6, 2006; DOI 10.1182/blood-2006-02-002204.

Supported by a Grant-in-Aid for Research of the Science Frontier Program and a Grant-in-Aid for Scientific Research from the Ministry of Education, Culture, Sports, Science, and Technology of Japan and by a Research Grant on Human Genome, Tissue Engineering (H17-014), from the Japanese Ministry of Health, Labor, and Welfare, Japan.

T.Y. designed and performed the research, analyzed the data, and wrote the paper; S.Y., Y.S., H. Miyatake, and T.U. performed the research; Y.M. analyzed the data and wrote the paper; M.I., H. Miyoshi, and S.K. provided vital reagents; T.H. analyzed the data; K.A. designed the research, analyzed the data, and wrote the paper.

The online version of this article contains a data supplement.

Reprints: Kiyoshi Ando, Department of Hematology, Tokai University School of Medicine Bohseidai, Isehara, Kanagawa 259-1193, Japan; e-mail: andok@keyaki.cc.u-tokai.ac.jp.

The publication costs of this article were defrayed in part by page charge payment. Therefore, and solely to indicate this fact, this article is hereby marked "advertisement" in accordance with 18 U.S.C. section 1734.

Analyzing the thymus-repopulating activity of these cells provides a unique way to distinguish and identify long-term self-renewing stem cells within the SRC's. Self-renewal of HSC's has been assessed by serial transplantation on the basis that HSC's, which are responsible for multilineage hematopoiesis in primary recipients, are also capable of repeating this process in secondary transplant recipients. Confirmation of the persistence of thymus-repopulating cells with multilineage differentiation ability in the secondary recipient would eliminate the possible contribution of some long-lived progenitors and mature cells and at the same time, provide direct evidence for self-renewal of SRC's.

In this study, we established a novel strategy to analyze both self-renewal and multilineage differentiation of a single human thymus-repopulating SRC clone in NOG recipient mice using linear amplification-mediated polymerase chain reaction (LAM-PCR) that verifies individual genomic virus integration sites by direct sequencing.[23] The identification of specific clones in fluorescent-activated cell sorter (FACS)–sorted lymphomyeloid lineage populations by their unique molecular markers allowed us to assess how individual clones contribute to the specific lineages during long-term hematopoiesis in vivo. We focused on CD4/CD8 double-positive (DP) immature thymocyte populations as a starting point of our clonal analysis of the human HSC ability. Our study presented direct clonal evidence that a single human HSC had the ability to produce lymphoid and myeloid lineage cells. Self-renewal division of multilineage clones resulted in expansion of SRC's. However, this clonal expansion of SRC's leads to the clonal exhaustion of SRC's during long-term hematopoiesis in vivo. It was also indicated that, although most of the SRC clones were destined to loose their self-renewal potential, the relatively small proportion of SRC clones retained extensive self-renewal potential.

Materials and methods

Collection and purification of human CB CD34$^+$CD38$^-$ cells

CB samples were obtained from full-term deliveries according to the institutional guidelines approved by the Tokai University Committee on Clinical Investigation. Mononuclear cells (MNCs) were isolated by Ficoll-Hypaque (Lymphoprep, 1.077 ± 0.001 g/mL; Nycomed, Oslo, Norway) density gradient centrifugation. CD34$^+$ cell fractions were prepared using the CD34 Progenitor Cell Isolation Kit (Miltenyi Biotec, Sunnyvale, CA) according to the manufacturer's directions. Column-enriched CD34$^+$ cells were cryopreserved in liquid nitrogen until use. For isolation of CD34$^+$CD38$^-$ cells, pooled CD34$^+$-enriched cells from multiple donors were stained with fluorescein isothiocyanate–conjugated anti-CD34 (581; Coulter/Immunotech, Marseille Cedex, France), and phycoerythrin (PE)–conjugated anti-CD38 (HB7; BD Biosciences, San Jose, CA) monoclonal antibodies (mAbs). Cells were sorted using the FACSVantage flow cytometer (BD Biosciences) equipped with HeNe and argon lasers. CD38$^-$ gate was determined in reference to isotype control. CD34$^+$CD38$^-$ cells, which comprise 5% to 8% of the total CD34$^+$ cell population, were isolated with 97% to 99% (n = 16) purity using FACSVantage (BD Biosciences).

Lentivirus infection

Purified CD34$^+$CD38$^-$ cells were plated on fibronectin CH-296 fragment and incubated with highly concentrated viral supernatant at a multiplicity of infection (MOI) of 50 in serum-free StemPro-34 medium (Invitrogen, Carlsbad, CA) containing cytokines (Takara Shuzo, Tokyo, Japan) for 16 hours. Recombinant human thrombopoietin (50 ng/mL; kindly donated by Kirin Brewery, Tokyo, Japan), stem cell factor (50 ng/mL; donated by Kirin Brewery, Tokyo, Japan), and Flk-2/Flt-3 ligand (50 ng/mL; R&D Systems, Minneapolis, MN) were used. The number of virus integration sites per cell was examined in the following experiment. CD34$^+$ cells were infected with enhanced green fluorescent protein (EGFP) at an MOI of 50 and then plated in methylcellulose. Individual colonies expressing EGFP were picked up and analyzed for integration sites by LAM-PCR. Over the 20 colonies examined, none of the colonies demonstrated multiple bands, confirming that the individual colonies contain a single integration site (data not shown).

Estimation of multilineage differentiation potential of SRCs

NOD/Shi-scid, IL-2Rγc^{null} (NOG) mice were obtained from the Central Institute for Experimental Animals (Kawasaki, Japan) and maintained in the animal facility of the Tokai University School of Medicine in microisolator cages; the animals were fed with autoclaved food and water. Nine- to 20-week-old NOG mice were irradiated with 250 cGy X-rays. The following day, transduced CD34$^+$CD38$^-$ cells (1×10^4 cells) were injected intravenously into the NOG mice. All experiments were approved by the animal care committee of Tokai University. Sixteen to 20 weeks after transplantation, the mice were humanly killed, and bone marrow (BM) cells, splenocytes, and thymocytes were analyzed by flow cytometry. Cells were stained with mAbs to human leukocyte differentiation antigens. Human hematopoietic cells were distinguished from mouse cells by the expression of human CD45. APC-conjugated anti–human CD19 mAb (Coulter/Immunotech), ECD-conjugated anti–human CD8 and CD34 mAbs (all Coulter/Immunotech), and PE-conjugated anti–human CD3, CD4, and CD33 mAbs were used. The efficiency of gene transduction was determined by the percentage of cells expressing EGFP. EGFP-expressing CD45$^+$ human hematopoietic cells were further classified into human stem/progenitor (CD34$^+$), myeloid (CD33$^+$), B-lymphoid (CD19$^+$), and T-lymphoid (CD3$^+$ or CD4$^+$/CD8$^+$) subpopulations and were sorted using a FACSvantage Diva option (BD Biosciences). To eliminate the contamination of lineage-committed cells, CD34$^+$ cells were sorted on CD19$^-$ and CD33$^-$ gate. Sorted cells, confirmed to be lineage^{low}CD34$^+$, were designated as stem/progenitor cells. Double cell-sorting was performed to ensure greater than 99% cell purity. Representative FACS profiles of sorting purity were demonstrated in Figure S1 (available at the *Blood* website; see the Supplemental Materials link at the top of the online article).

Secondary transplantation

BM cells were obtained from mice that received a transplant with CD34$^+$CD38$^-$ cells at 13 to 19 weeks after transplantation. The BM cells of these primary recipients were divided equally and injected intravenously into 2 sublethally irradiated secondary NOG recipients (1.35×10^7–2.1×10^7 cells per recipient). Thirteen to 19 weeks after transplantation, BM cells and thymus were collected from each secondary recipient and used for flow cytometric analysis and lineage cell sorting as described.

Integration site analysis of lentivirally marked SRCs

LAM-PCR was carried out as described previously[24] with some slight modifications. Genomic DNA samples (100 ng), isolated from each sorted subpopulation, were preamplified for a total of 100 cycles by repeated primer extension using 0.25 pmol vector-specific, 5′-biotinylated primer LTR1 (5′-GAACCCACTGCTTAAGCCTCA-3′) using ProofStart DNA polymerase (2.5U; Qiagen, Hilden, Germany). The biotinylated extension products were collected using streptavidin-conjugated magnetic beads (Dynal, Oslo, Norway), and the second strand was synthesized using Klenow polymerase (2 U; Takara Shuzo) and random primer (Takara Shuzo). To prevent virus-vector sequence contamination, samples were first incubated with SacI endonuclease (5 U; Promega, Madison, WI) for 2 hours at 37°C and then digested with Tsp509I endonuclease (5 U; New England Biolabs, Ipswich, MA) for 2 hours at 65°C. After restriction digestion, 100 pmol of a linker cassette (5′-GTAATACGACTCACTATAGGGAGA-3′) was ligated using a DNA ligation kit (Takara Shuzo) at 16°C overnight. Each ligated sample was amplified using a vector-specific primer, LTR2 (5′-AGCTTGGCTTGAGTGCTTCA-3′),

and a linker cassette primer (5′-GTACATATTGTCGTTAGAACGCGTA-ATACGACTCA-3′), using the following conditions: 95°C for 1 minute, 60°C for 1 minute, 72°C for 1 minute (30 cycles). Each PCR product was subjected to nested PCR with the internal primers, LTR3 (5′-AGTAGTGTGTGCCCGTCTGT-3′) and LC2 (5′-CGTTAGAACGCGTA-ATACGACTCACTATAGGGAGA-3′), under identical conditions. PCR products were sequenced after cloning into the TOPO TA cloning vector (Invitrogen). The proviral integration sites of DP cells were sequenced, and the sequences were examined for alignment to the human genome using NCBI BlastN (http://www.ncbi.nlm.nih.gov/blast). The verified genomic sequence information of these DP cell integration sites was used to design new primers (all primer sequences used in this study are listed in Tables S1-S3). PCR was performed on each LAM-PCR product using the unique genomic flanking primers in combination with the LTR3 primers.

Estimation of clone size by real-time quantitative PCR (RQ-PCR)

Genomic DNA samples from CD34$^+$ cells of secondary recipients were amplified using multiple displacement amplification reagents (REPLI-g; Qiagen) according to the manufacturer's instructions.[25] Briefly, 10 ng template DNA was mixed with the DNA polymerase and incubated for 16 hours at 30°C. Approximately 50 μg amplified DNA was obtained from each sample. For RQ-PCR, each target DNA was amplified on the same plate with β-globin as the reference using the QuantiTect SYBR Green PCR Master Mix (Qiagen) and the ABI Prism 7700 Sequence Detection System (Applied Biosystems). The relative clone amounts and range were determined in reference to β-globin. Threshold cycles (C_T) were determined as to fit all samples in logarithmic phase. To ensure the efficiency of amplification and the assay precision, calibration curves for each clone sequence were constructed to have the correlations (r^2) of above 0.95 and the efficiency of greater than 98%. A comparative C_T was used to determine the proportion of CD34$^+$ clones in paired secondary recipients that were derived from the parent primary recipient clone. For each sample, the clone C_T value was normalized using the formula $\Delta C_T = \Delta C_T$ clone $- \Delta C_T$ β-globin. To determine relative clone size, the following formula was used: $\Delta\Delta C_T = \Delta C_T$ clone in CD34+ cells of the one secondary recipient $- \Delta C_T$ clone in CD34+ cells of the other secondary recipient, and the value was calculated by the expression $2^{-\Delta\Delta CT}$. Each reaction was performed at least in triplicate. Amplification conditions were as follows: 95°C for 15 minutes followed by 40 cycles at 95°C for 15 seconds, 60°C for 30 seconds, and 72°C for 60 seconds.

The same primer set described in PCR tracking of LAM-PCR procedure was used to amplify each clone. As an internal control, human hematopoietic cell kinase 1 (*HCK1*) gene and ribosomal DNA (*rDNA*) gene were also amplified. Even amplification of each genomic DNA was confirmed by RQ-PCR using all 3 internal control primers (data not shown).[26] The primers for β-globin gene were forward, 5′-GTGCACCTGACTCCTGAG-GAGA-3′, and reverse, 5′-CCTTGATACCAACCTGCCCAG-3′. Primers for *HCK1* gene were forward, 5′-TATTAGCACCATCCATAGGAGGCTT-3′, and reverse, 5′-GTTAGGGAAAGTGGAGCGGAAG-3′. Primers for *rDNA* gene were forward, 5′-CCATCGAACGTCTGCCCTA-3′, and reverse, 5′-TCACCCGTCGTCACCATG-3′.

Statistical analysis

Data are represented as mean ± SD. The 2-sided P value was determined by testing the null hypothesis that the 2 population medians are equal. P values less than .05 were considered to be significant.

Results

Multilineage differentiation of gene-marked SRCs

To investigate the multilineage differentiation and self-renewal capacity of individual SRC clones, we introduced recombinant lentiviral vector carrying an EGFP-encoding gene to cord blood CD34$^+$CD38$^-$ cells which can provide long-term engraftment (more than 12 weeks) and multilineage differentiation,[2] and then we transplanted these cells into sublethally irradiated NOG mice. Multilineage differentiation was determined as the proportion of each hematopoietic lineage within the EGFP-expressing human CD45$^+$ cell population using FACS at 16 to 20 weeks after transplantation (Figure 1). Consistent with our previous results,[16] substantial engraftment, including CD34$^+$ primitive cells, CD33$^+$ myeloid, CD19$^+$ B-lymphoid, CD3$^+$ mature, and DP immature T-lymphoid cells, was observed in the BM, spleen, and thymus of the NOG mice (Table 1). Because the proportion of nontransduced EGFP$^-$ cells within the human graft and the percentage of EGFP$^+$ cells within each lineage were not significantly different (data not shown), these data indicated that EGFP transduction did not affect the differentiation and proliferation capacity of the SRCs.

Multilineage differentiation of individual thymus-repopulating SRC clones

To analyze the multilineage differentiation capacity of individually transduced SRCs, we performed in vivo integration site analysis by LAM-PCR that can distinguish the progeny of each transduced cell

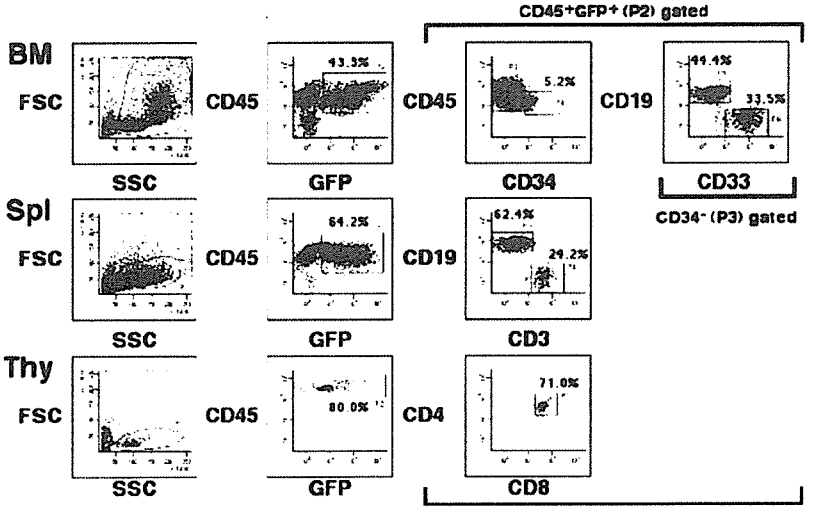

Figure 1. Representative FACS profiles of EGFP-transduced SRCs. Samples were obtained from BM, spleen, and thymus of a NOG mouse, and the proportion of EGFP-transduced human cells was evaluated. The relative frequencies of each cell population are indicated.

Table 1. Proportion of each human cell lineage engrafted in primary NOG mice

Mouse	Week*	Bone marrow, % engrafted					Spleen, % engrafted				Thymus, % engrafted		
		CD45	EGFP	S	M	B	CD45	EGFP	T	B	CD45	EGFP	T
1	17	82.2	84.8	22.1	4.6	ND	81.8	65.3	2.1	88.6	97.8	83.0	82.6
3	17	74.0	58.5	5.2	33.5	44.4	82.1	78.2	24.2	62.4	85.5	80.0	71.0
4	16	88.9	75.4	8.5	17.5	64.4	75.6	77.9	1.6	87.9	95.0	52.9	23.4

The total cellularity of BM and thymus in the primary recipient was 3.56 10^7 ± 0.53 10^7 and 1.39 10^5 ± 1.13 10^5, respectively. Each mouse listed in the table received a transplant of 10 10^3 $CD34^+CD38^-$ cells.

S indicates $CD34^+$ stem/progenitor cells; M, $CD33^+$ myeloid lineage cells; B, $CD19^+$ B lymphoid lineage cells; T, $CD3^+$ (spleen) or CD4/CD8 double-positive (thymus) T-lymphoid lineage cells; ND, not done.

*Weeks after transplantation. Bone marrow cells, spleen cells, and thymocytes of NOG mice were stained with an anti–human CD45 mAb and analyzed. The proportion of EGFP-expressing cells within the $CD45^+$ cells and cells positive for each lineage marker in the $CD45^+/EGFP^+$ was calculated.

by its unique proviral-genomic fusion sequence (Figure 2A). Direct sequencing of PCR products derived from $EGFP^+CD45^+$ DP cells verified that each product with a unique band length represented individual and different clones. LAM-PCR analysis of $EGFP^+CD45^+$ FACS-purified lineage populations detected multiple integration sites in each cell lineage (Figure 2B). It is reported that the number of vector copies per cell can be controlled by adjusting the MOI, without reducing the transgene expression levels.[27] Because we optimized the experimental conditions to have each cell carrying one insertion per cell, confirmed by both colony-forming assay (see "Materials and methods") and transplantation assay,[24] multiple integration sites detected by LAM-PCR indicated polyclonal repopulation in the NOG mice.

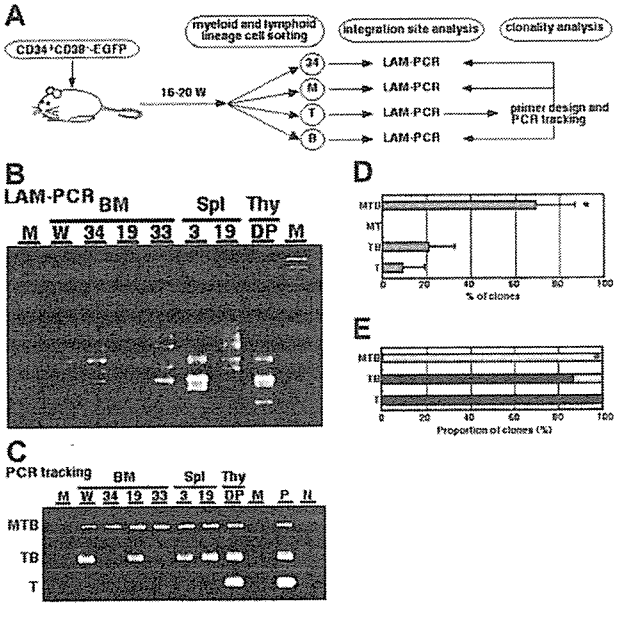

Figure 2. Clonal analysis of primary transplanted SRCs. (A) Study design for clonal analysis of primary grafts. 34 indicates $CD34^+$ stem/progenitor cells; M, $CD33^+$ myeloid lineage cells; B, $CD19^+$ B-lymphoid lineage cells; T, $CD3^+$ (spleen) or CD4/CD8 double-positive (thymus) T-lymphoid lineage cells. (B) Representative LAM-PCR profiles of SRCs. Each band represents a different insertion locus in the assayed material. W indicates unseparated whole BM MNCs; M, size marker. (C) DP-derived T-lymphoid insertion sites were traced by PCR. The clones detected in all lymphomyeloid lineage cells were designated as multipotent type (MTB). TB indicates clones restricted in T lymphoid and B lymphoid cells; T, clones detected in T-lymphoid cells; W, unseparated whole BM MNCs; M, size marker; P, TA-cloned LAM-PCR product was used as a positive control; N, DW. (D) Relative frequencies of each clone type detected in primary SRCs. Data represent mean ± SD of 3 independent experiments. $^*P < .01$ relative to other type of clones. (E) The proportion of clones detected in the $CD34^+$ cell population. A total of 27 clones in 3 independent experiments were analyzed. Gray bars represent the clones detected in $CD34^+$ cells. Black bars represent the clones not detected in $CD34^+$ cells. $^*P < .01$ relative to other type of clones.

A total of 27 clones were identified in 3 independent experiments based on the genomic sequence information of the LAM-PCR products from the DP cells (Table S1 summarizes the results of the integration site analysis of DP cells). Using primers designed to correspond to individual integration sites, and therefore unique clones, we were able to track the individual clones and their progenies, including $CD34^+$ stem/progenitor, myeloid, and B-lymphoid cells (Figure 2A). Three different clone types were observed in this experiment (Figure 2C): a multipotent type (MTB), in which insertion sites originally detected in the DP cells were also detected in the highly purified myeloid and B-lymphoid cell populations; a unipotent progenitor containing exclusively T cells; and a bipotent T/B progenitor. However, a bipotent progenitor containing myeloid and T lymphocytes was not detected. As expected, analysis of thymus-repopulating cells revealed that the majority of SRC clones (70.4%) found in the recipient mice were of the MTB multilineage type (Figure 2D; Table 2). We also used CD14 and CD66b, a more mature myeloid marker, for clonal analysis and detected the equivalent proportion of the 3 clone types (data not shown). Interestingly, all MTB clones were found in the $CD34^+$ cell population (Figure 2E), suggesting that the transduced SRC clones self-replicated within the $CD34^+$ stem cell pool without losing their ability to contribute to both lymphoid and myeloid lineages during long-term hematopoiesis. However, as the differentiation capacity of clones became limited to bipotency or unipotency, the proportion of clones that were also found in the $CD34^+$ cell population decreased (Figure 2E), indicating that some SRC clones had been exhausted from the stem cell pool during lineage commitment.

In vivo expansion of individual thymus-repopulating SRC clones

To directly demonstrate the self-renewal capacity of the SRCs, we injected BM cells from each primary mouse into 2 secondary mice

Table 2. Differentiation potential of thymus-repopulating SRC clones

Mouse	No. of clones	Clone type, no. (%)		
		MTB	TB	T
1	5	3 (60)	1 (20)	1 (20)
3	12	7 (58.3)	4 (33.3)	1 (8.3)
4	10	9 (90)	1 (10)	0 (0)
Total	27	19 (70.4)	6 (22.2)	2 (7.4)

Lineage contribution of individual thymus-repopulating SRC clones was evaluated by PCR tracking based on integration site analysis of DP cells. No clones were differentiated into M and T lineages.

MTB indicates clones that gave rise to myeloid (M), T lymphoid (T), and B lymphoid (B) lineages; TB, clones differentiated into T and B lineages; T, clones differentiated into T lineage only.

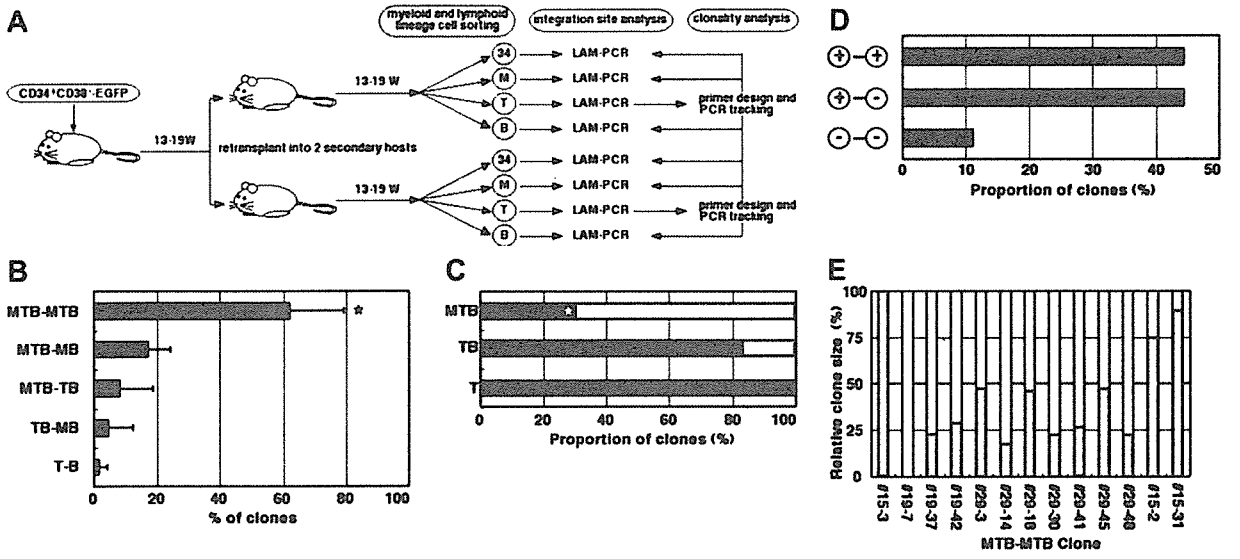

Figure 3. Clonal analysis of secondary transplanted SRCs. (A) Study design for clonal analysis of secondary grafts. 34 indicates CD34+ stem/progenitor cells; M, CD33+ myeloid lineage cells; B, CD19+ B-lymphoid lineage cells; T, CD3+ (spleen) or CD4/CD8 double-positive (thymus) T-lymphoid lineage cells. (B) Relative frequencies of each clone type detected in paired secondary transplanted recipients. Data represent mean ± SD of 3 independent experiments. *$P < .01$ relative to other type of clones. (C) The proportion of clones detected in CD34+ cells is shown. A total of 43 clones in 3 independent experiments were analyzed. Gray bars represent the clones detected in CD34+ cells. Black bars represent the clones not detected in CD34+ cells. *$P < .01$ relative to MTB clones found in primary recipients (shown in Figure 1E). (D) The proportion of MTB clones found in CD34+ cells of paired secondary recipients. A total of 27 clones in 3 independent experiments were analyzed. Notation of the left vertical axis: +/+, MTB-MTB clone pairs were detected in CD34+ cells of both secondary recipient pairs; +/−, MTB-MTB clone pairs were detected in the CD34+ cells of 1 of the 2 secondary recipient pairs; and −/−, MTB-MTB clone pairs were not detected in the CD34+ cells of either secondary recipient pairs. (E) Relative clone size of individual clones in each MTB-MTB clone pairs in CD34+ stem cell pool found in paired secondary recipient. The relative clone size of individual clones in 11 MTB-MTB clone pairs detected in CD34+ cells of both secondary recipients was examined by RQ-PCR. The relative clone size of individual clones in each MTB-MTB pair is expressed as the proportion of one clone relative to the other clone. The MTB-MTB clone pairs no.15-3 and no. 19-7 that was detected in the CD34+ cells of only 1 of the 2 secondary recipient pairs were used as experimental control and demonstrated complete skewing to either one recipient.

(Figure 3A). Although each primary BM cell population was divided into 2 recipients, substantial engraftment was observed in these secondary-recipient NOG mice (Table 3). Clone tracking analysis was then performed to examine the fate of individual SRC clones in paired secondary mice. Integration site analysis by LAM-PCR of FACS-sorted cells showed polyclonal reconstitution in each secondary host. A total of 43 clones were identified by integration site analysis of DP T lymphocytes found in 3 secondary recipient pairs (results are summarized in Table S2). All clones detected in paired secondary recipients were also detected in the primary donor. Strikingly, all 43 clones were found as a pair; clones detected in one of the secondary recipient pairs were always observed in the other pair. In greater than 90% of these clone pairs (39 of 43), at least 1 of the daughter clones inherited MTB differentiation potential from its parent clone. Moreover, in 69.2% of these 39 clone pairs, both daughter clones remained multipotent (MTB-MTB type), whereas the other daughter clone in the remaining 30.8% of clone pairs became committed to specific cell lineages (MTB-MB or MTB-TB type) (Figure 3B; Table 4). The existence of MTB-MTB type clones in secondary recipients indicated that a single SRC clone self-replicated in the primary recipients and produced 2 daughter clones that retained SRC potential, thereby resulting in the in vivo expansion of multipotent SRC clones.

Table 3. Proportion of the primary and the secondary human graft

Mouse	Cell dose*	Week†	Bone marrow, %					Thymus, %		
			CD45	EGFP	S	M	B	CD45	EGFP	T
Primary recipient										
101	17	13	80.3	72.7	ND	ND	ND	ND	ND	ND
109	6	19	66.2	71.0	ND	ND	ND	ND	ND	ND
113	10	14	43.2	71.8	ND	ND	ND	ND	ND	ND
Secondary recipient										
101-1	21	13	63.0	93.3	3.4	7.4	63.7	98.2	80.1	83.6
101-2	21	13	62.5	88.1	4.2	14.6	54.9	96.5	78.6	71.2
109-1	13.5	17	29.4	69.4	1.3	49.5	29.9	91.3	78.2	90.5
109-2	13.5	17	33.3	75.1	1.9	27.6	45.9	93.0	70.1	81.1
113-1	19.3	19	72.3	68.7	3.4	17.3	38.7	95.5	88.1	88.0
113-2	19.3	19	86.3	50.0	0.6	17.2	17.3	92.9	72.3	70.3

The total cellularity of BM in the primary and the secondary recipient was $3.86 \times 10^7 \pm 0.83 \times 10^7$ and $3.72 \times 10^7 \pm 0.91 \times 10^7$, respectively. The total cellularity of thymus in the primary and the secondary recipient was $3.36 \times 10^5 \pm 3.28 \times 10^5$ and $2.43 \times 10^5 \pm 1.59 \times 10^5$, respectively.

ND indicates not done.

*Number of CD34+CD38− cells transplanted (primary recipient, 10^5; secondary recipient, 10^6)

†Number of weeks after transplantation

Table 4. Differentiation potential of paired secondary clones

Mouse	No. of clones	Clone type, no. (%)				
		MTB-MTB	MTB-MB	MTB-TB	MB-TB	T-B
101	22	12 (54.5)	5 (22.7)	1 (4.5)	3 (13.6)	1 (4.4)
109	11	9 (81.8)	2 (18.2)	0 (0)	0 (0)	0 (0)
113	10	6 (60)	2 (20)	2 (20)	0 (0)	0 (0)
Total	43	27 (62.8)	9 (20.9)	3 (7)	3 (7)	1 (2.3)

Differentiation potential of paired secondary clones was determined by PCR tracking strategy based on integration site analysis of DP cells developed in secondary recipients.

Individual thymus-repopulating SRC clones have different self-renewal capacities

Consistent with our earlier observations in the primary recipient mice, the proportion of MTB clones present in the $CD34^+$ cell population decreased as the differentiation capacity of the clones became limited (Figure 3C). In addition, note that 30.3% of MTB clones in the secondary recipient mice were no longer found in the $CD34^+$ cell population, contrasting with the initial finding that all MTB clones in the primary mice were found in the $CD34^+$ cell population (Figure 2E). Therefore, phenotypic and possibly functional differences exist between MTB clones in the primary and secondary recipient mice, although both were capable of repopulating and giving rise to multilineage progenitors in the host. To assess how the MTB clone cell division affected the status of daughter MTB clones, we examined how many of in vivo–expanded MTB-MTB clone pairs were also found in the $CD34^+$ cell population and classified into 3 groups (Figure 3D). First, in 44.4% of the MTB-MTB clone pairs, both daughter clones were found in the $CD34^+$ cell population. Second, in another 44.4% of MTB-MTB clone pairs, only one of the daughter clones was found in the $CD34^+$ cell population. These results indicated that the former type clones have relatively higher SRC activity and that, as a result of unequal distribution of SRC activity in 2 daughter clones after cell division, 1 of the daughter clones exited from the $CD34^+$ stem cell pool. Finally, in 11.1% of MTB-MTB clone pairs, neither daughter clone was detected in the $CD34^+$ stem cell pool, which may reflect the extensive replication required to repopulate both primary and secondary recipients that eventually leads to exhaustion of the stem cells. These results demonstrate the heterogeneity among clones that repopulate both the primary and secondary recipient mice.

To further confirm our findings of heterogeneity of SRC clones, we quantitatively examined what was the relative clone size ratio of each MTB-MTB clone pair in the $CD34^+$ stem cell pool by RQ-PCR. In the majority of MTB-MTB clone pairs, the proportion of individual clone in each clone pair varied widely (Figure 3E). Interestingly, only a small proportion of MTB-MTB clone pairs (no. 29-3, no. 29-18, and no. 29-45) were found to be equally distributed to each paired recipient. Those clone pairs that were able to repopulate equally in a paired secondary recipient may have more extensive self-renewal capacity. The results indicated that individual thymus-repopulating SRC clones have different self-renewal capacities, which is a basis for a hierarchically organized stem cell pool.

We also performed tertiary transplantation and analyzed SRC clones found in the recipients. The level of engraftment in tertiary recipients was less than 1% in BM and 0.1% in the thymus ($n = 4$). We performed integration site analysis on unseparated BM MNCs of tertiary recipients and obtained 17 clones from 4 mice. The status of individual tertiary SRC clones in the secondary recipients was examined by clone tracking analysis using the LAM-PCR products from tertiary graft as a starting point of clonal analysis. We found that all SRC clones in the tertiary mice were detected in the $CD34^+$ stem cell pool of secondary recipient (Table S3 summarizes the results of the integration site analysis of SRCs). The results of tertiary transplantation experiment confirmed that only HSC clones that continuously replicate themselves in the $CD34^+$ stem cell pool could produce descendents to maintain long-term hematopoiesis.

Discussion

This study provides the first direct evidence for the multilineage differentiation and self-renewal of human HSCs at the single-cell level in vivo using PCR tracing analysis of individual thymus-repopulating clones. We demonstrated that polyclonal thymus-repopulating clones with multilineage differentiation and self-renewal abilities were able to maintain long-term human hematopoiesis. This study revealed several features of human HSCs that are important biologically and clinically. First, self-renewal division of individual thymus-repopulating clones resulted in clonal expansion of cells with multilineage differentiation in vivo. Second, a single thymus-repopulating clone produced progeny that were heterogeneous in SRC activity. Third, as a result of continuous division and/or advancement of lineage commitment, some of these multipotent thymus-repopulating clones were destined to limit their capability for multilineage differentiation and self-renewal. Our study indicated that, although the majority of thymus-repopulating clones loose their self-renewal potential, a relatively small proportion of thymus-repopulating clones retain extensive self-renewal potential. Therefore, the self-renewal capacity distinctly different in individual thymus-repopulating clones may cause a hierarchically organized stem cell pool.

Controlling the copy number of the virus vector in each transduced cell is important for our clonality analysis. We recently reported the direct evidence for single virus integration per cell in a transplantation study.[24] When EGFP-transduced $CD34^+$ cells expanded in vitro were divided and transplanted into multiple recipient mice, the unique integration site representing individual clones were detected in multiple mice; in other words, multiple mice were engrafted with the same clone. If a cell contains more than one integration site and assessed as "different" clones, these different clones should be detected in the same recipients. However, none of the clones demonstrated the identical engraftment pattern. In addition, clonal tracking analyses in this study clearly demonstrated that the individual SRC clones were both qualitatively and quantitatively heterogenous. Everything being considered, our infection condition achieves one copy per cell. Even if there is a slight possibility that the number of copies per cell is more than one, the clonality is not denied. Because a virus gene integrates into the host genome at a random site, progenies having a common integration site are developed from a single clone. It could affect the numeric calculation of the number of clones, but it would not influence our interpretation of the result.

Although the concept of HSCs was proposed decades ago and is well accepted, little experimental data regarding multipotency of human HSCs is available. Using a genetic marking strategy in both experimental[6-12] and clinical studies,[28-33] it has been suggested that hematopoietic reconstitution after transplantation is attributed to oligoclonal or polyclonal HSC activity and that the repopulation capacity of individual HSCs is substantially heterogeneous. However, the results of these studies, such as the presence of transgene expression in B lymphocytes and myeloid cells and the detection of similar genomic bands in multiple hematopoietic recipient organs, were not sufficient to unequivocally determine the multipotency of human HSCs at the single-cell level. Recently, Schmidt et al[34] reported clonal evidence for multilineage

human hematopoietic differentiation from IL-2Rcγ gene-transduced CD34 cells transplanted into patients with X-linked SCID. Considering that the IL-2Rcγ has been known to play a critical role in lymphoid development,[35] the observations based on the IL-2Rcγ gene-expressing clone may not reflect authentic hematopoietic development because of possible lineage commitment redirection mediated by cytokines that act on IL-2Rcγ. Although the HSC's potential was elaborately assessed clonally in vitro,[36,37] there exists some concerns; the lineage commitment could be easily fluctuated by culture conditions; homing of HSCs to thymus was neglected. The field has thus far lacked experimental evidence showing that purified human HSCs possess the potential for multilineage differentiation at the single-cell level. In this study, we succeeded in demonstrating that a single HSC gave rise to myeloid, T-, and B-lymphoid lineage cells by using LAM-PCR–based clonal tracing analysis in highly purified lymphomyeloid cell populations. Our results now provide data supporting the multipotency of a single human HSC.

Transplantation of prospectively isolated donor cells in mice has demonstrated that only HSCs can sustain thymopoiesis for a long period.[38,39] A lack of reliable in vivo experimental models for human thymocyte reconstitution and clonal stem cell assays has precluded determining whether the same applies to human HSCs. In this study, we used the thymus-repopulating potential of individual SRC clones as a means to analyze human HSCs at a single-cell level in vivo. Previously, we have demonstrated that human T lymphocytes derived from CD34 cells and developed in NOG recipient mice bore polyclonal Vβ TCR and responded not only to mitogenic stimuli but also to allogeneic human cells, which reflects normal human T-lymphoid cell development.[16-19] By analyzing individual thymus-repopulating clones in the NOG recipient, we successfully demonstrated that human thymus-repopulating cells were derived from a single multipotent-type HSC clone and were capable of maintaining long-term thymopoiesis in vivo. This is the first clonal evidence that multipotent HSCs contribute to long-term human thymopoiesis.

Self-renewal is essential for HSCs to maintain homeostasis in the blood system by the sequential generation of mature blood cells throughout a lifetime. To maintain the total pool of HSCs, this ability must be passed on to at least one of the daughter cells in each division. If both daughter cells undergo terminal differentiation, HSCs will eventually be lost. On the other hand, if both daughter cells retain stem cell properties, the total number of HSCs will increase, resulting in expansion of HSCs.[40] In fact, an increase in the number of murine[41,42] (and human[43,44]) repopulating cells was reported in serial transplantation studies. Limiting dilution analysis showed that secondary recipients contained larger numbers of HSCs than was originally injected. These results suggest that HSCs can replicate vigorously under certain conditions. However, it has been shown that HSCs intrinsically limit their potential for self-renew.[45-47] Recently, Ema et al[48] observed the self-renewal ability of HSCs by single murine HSC serial transplantation experiments and statistically determined that the number of HSCs increased in the BM of recipients, although the mean activity of individual HSCs was reduced. Taken together, this finding suggests that, although HSCs replicate themselves, which results in expansion of HSCs, they sequentially loose their potential as a HSC. Our clonal analysis of thymus-repopulating cells in paired secondary recipients provides direct evidence to address this innate property of HSCs in vivo.

Our finding that the same multipotent HSC clone was detected in paired secondary recipients (MTB-MTB type) indicates that a single SRC clone can self-replicate to produce 2 daughter cells with multilineage differentiation and self-renewal potential, leading to the in vivo expansion of SRCs. It has been considered that SRCs that can engraft and give rise to multilineage cells in secondary recipients are self-renewed HSCs. Thus, these MTB-MTB clones in this study could be defined as HSCs. However, when the MTB-MTB clone pairs were further examined whether they remained in the stem cell pool, one of the daughter clones in the pair was no longer found in the CD34 cell population in approximately half of MTB-MTB clone pairs. Furthermore, the stem cell phenotype was not retained in 11.1% of MTB-MTB clones. Considering that 100% of MTB clones in primary recipients possess the stem cell phenotype, these results indicate that SRCs with the stem cell phenotype progressively decrease during serial transplantation, leading to exhaustion of SRCs. This is consistent with our finding that the proportion of clones with the stem cell phenotype decreased as the clone committed to specific lineages. By assessing the phenotype of self-replicated multilineage clone pairs, determined by the presence of common integration site in CD34 cell population, we were able to reveal the status of HSCs during aging. The loss of stem cell phenotype may be caused by extensive replication required for hematopoietic reconstitution in recipient. Although the total SRC population appears to expand, our data indicate that the ability of individual SRCs, in more than half of the clones, may become restricted during long-term hematopoiesis in vivo.

Our clonal tracking analysis clearly demonstrated that heterogeneity in the self-renewal capacity of individual multipotent SRC clones underlies the differences of clonal longevity in the stem cell pool (Figure 4). Although most of the SRC clones loose their self-renewal potential, a relatively small proportion of SRC clones

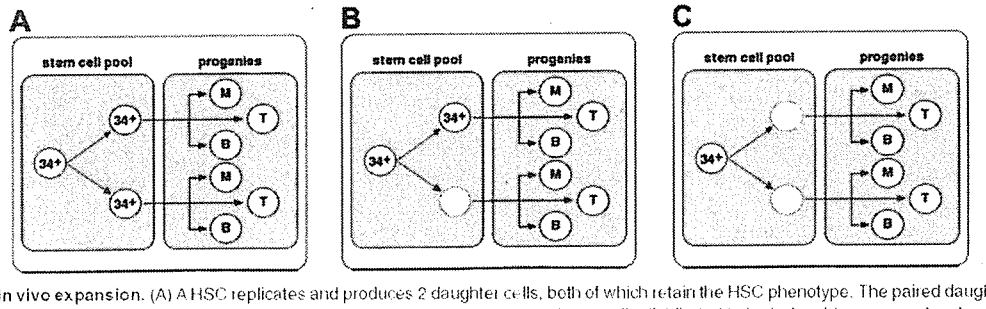

Figure 4. Schema of in vivo expansion. (A) A HSC replicates and produces 2 daughter cells, both of which retain the HSC phenotype. The paired daughter HSCs in the stem cell pool contribute to hematopoiesis; even so, the self renewal activity of the parent HSC may be equally distributed to both daughters or may be skewed to either daughter cell. (B) As a result of heterogeneous HSC replication, one of the daughter HSCs loses the stem cell potential and therefore exits from the stem cell pool, but still remains in the progenitor pool. (C) Both paired daughter cells have lost their HSC potential leading to exhaustion from the stem cell pool. 34 indicates CD34 stem/progenitor cells; M, CD33 myeloid lineage cells; B, CD19 B lymphoid lineage cells; T, CD3 (spleen) or CD4/CD8 double positive (thymus) T lymphoid lineage cells.

(3 of 43 total secondary descending clones) are able to continuously self-renew. Our strategy which combined lineage-cell sorting and LAM-PCR enabled identification of the MTB clone that continuously self-renews in the stem cell pool and represents the long-term HSC. Our study provides a method that can accurately evaluate in vivo properties of human HSCs, and further studies may lead to elucidation of the mechanisms of self-renewal of the long-term human HSC at the single-cell level. It has been demonstrated that long-term leukemic stem cells have extensive self-renewal potential, and their hierarchic organization of stem cell pool was notably similar to the normal HSC compartment.[49,50] These findings propose the idea that some forms of leukemia imitate a system of the normal long-term HSC and retain or acquire the extensive self-renewal capacity. The clonal analysis for properties of long-term HSCs in vivo will be a powerful tool to understand the mechanisms for tumor initiation, progression, and relapses and will lead to efficient use of HSCs in clinical transplantation medicine.

Acknowledgments

We thank Tadayuki Sato, Hideyuki Matsuzawa, and Hideo Tsukamoto of the Teaching and Research Support Center of Tokai University for technical assistance; members of the animal facility of Tokai University, especially Mayumi Nakagawa, for meticulous care of the experimental animals; and members of the Tokai Cord Blood Bank for their assistance. We also thank members of the Research Center for Regenerative Medicine of Tokai University for helpful discussion and assistance.

References

1. Larochelle A, Vormoor J, Hanenberg H, et al. Identification of primitive human hematopoietic cells capable of repopulating NOD/SCID mouse bone marrow: implications for gene therapy. Nat Med. 1996;2:1329-1337.
2. Bhatia M, Wang JC, Kapp U, Bonnet D, Dick JE. Purification of primitive human hematopoietic cells capable of repopulating immune-deficient mice. Proc Natl Acad Sci U S A. 1997;94:5320-5325.
3. Wang JC, Doedens M, Dick JE. Primitive human hematopoietic cells are enriched in cord blood compared with adult bone marrow or mobilized peripheral blood as measured by the quantitative in vivo SCID-repopulating cell assay. Blood. 1997;89:3919-3924.
4. Osawa M, Hanada K, Hamada H, Nakauchi H. Long-term lymphohematopoietic reconstitution by a single CD34-low/negative hematopoietic stem cell. Science. 1996;273:242-245.
5. Lemischka IR, Jordan CT. The return of clonal marking sheds new light on human hematopoietic stem cells. Nat Immunol. 2001;2:11-12.
6. Woods NB, Fahlman C, Mikkola H, et al. Lentiviral gene transfer into primary and secondary NOD/SCID repopulating cells. Blood. 2000;96:3725-3733.
7. Guenechea G, Gan OI, Dorrell C, Dick JE. Distinct classes of human stem cells that differ in proliferative and self-renewal potential. Nat Immunol. 2001;2:75-82.
8. Ailles L, Schmidt M, Santoni de Sio FR, et al. Molecular evidence of lentiviral vector-mediated gene transfer into human self-renewing, multipotent, long-term NOD/SCID repopulating hematopoietic cells. Mol Ther. 2002;6:615-626.
9. Piacibello W, Bruno S, Sanavio F, et al. Lentiviral gene transfer and ex vivo expansion of human primitive stem cells capable of primary, secondary, and tertiary multilineage repopulation in NOD/SCID mice. Nonobese diabetic/severe combined immunodeficient. Blood. 2002;100:4391-4400.
10. Barquinero J, Segovia JC, Ramirez M, et al. Efficient transduction of human hematopoietic repopulating cells generating stable engraftment of transgene-expressing cells in NOD/SCID mice. Blood. 2000;95:3085-3093.
11. Josephson NC, Vassilopoulos G, Trobridge GD, et al. Transduction of human NOD/SCID repopulating cells with both lymphoid and myeloid potential by foamy virus vectors. Proc Natl Acad Sci U S A. 2002;99:8295-8300.
12. Nagy KZ, Laufs S, Gentner B, et al. Clonal analysis of individual marrow-repopulating cells after experimental peripheral blood progenitor cell transplantation. Stem Cells. 2004;22:570-579.
13. Borrello MA, Phipps RP. The B/macrophage cell: an elusive link between CD5+ B lymphocytes and macrophages. Immunol Today. 1996;17:471-475.
14. Hou YH, Srour EF, Ramsey H, Dahl R, Broxmeyer HE, Hromas R. Identification of a human B-cell/myeloid common progenitor by the absence of CXCR4. Blood. 2005;105:3488-3492.
15. Ito M, Hiramatsu H, Kobayashi K, et al. NOD/SCID/gamma(c)(null) mouse: an excellent recipient mouse model for engraftment of human cells. Blood. 2002;100:3175-182.
16. Yahata T, Ando K, Nakamura Y, et al. Functional human T lymphocyte development from cord blood CD34+ cells in nonobese diabetic/Shi-scid, IL-2 receptor gamma null mice. J Immunol. 2002;169:204-209.
17. Hiramatsu H, Nishikomori R, Heike T, et al. Complete reconstitution of human lymphocytes from cord blood CD34+ cells using the NOD/SCID/gammacnull mice model. Blood. 2003;102:873-880.
18. Scollay R, Smith J, Stauffer V. Dynamics of early T cells: prothymocyte migration and proliferation in the adult mouse thymus. Immunol Rev. 1986;91:129-157.
19. Bhandoola A, Sambandam A, Allman D, Meraz A, Schwarz B. Early T lineage progenitors: new insights, but old questions remain. J Immunol. 2003;171:5653-5658.
20. Glimm H, Eisterer W, Lee K, et al. Previously undetected human hematopoietic cell populations with short-term repopulating activity selectively engraft NOD/SCID-beta2 microglobulin-null mice. J Clin Invest. 2001;107:199-206.
21. Hogan CJ, Shpall EJ, Keller G. Differential long-term and multilineage engraftment potential from subfractions of human CD34+ cord blood cells transplanted into NOD/SCID mice. Proc Natl Acad Sci U S A. 2002;99:413-418.
22. Mazurier F, Doedens M, Gan OI, Dick JE. Rapid myeloerythroid repopulation after intrafemoral transplantation of NOD-SCID mice reveals a new class of human stem cells. Nat Med. 2003;9:959-963.
23. Schmidt M, Hoffmann G, Wissler M, et al. Detection and direct genomic sequencing of multiple rare unknown flanking DNA in highly complex samples. Hum Gene Ther. 2001;12:743-749.
24. Ando K, Yahata T, Sato T, et al. Direct evidence for ex vivo expansion of human hematopoietic stem cells. Blood. 2006;107:3371-3377.
25. Dean FB, Hosono S, Fang L, et al. Comprehensive human genome amplification using multiple displacement amplification. Proc Natl Acad Sci U S A. 2002;99:5261-5266.
26. Hosono S, Faruqi AF, Dean FB, et al. Unbiased whole-genome amplification directly from clinical samples. Genome Res. 2003;13:954-964.
27. Mazurier F, Gan OI, McKenzie JL, Doedens M, Dick JE. Lentivector-mediated clonal tracking reveals intrinsic heterogeneity in the human hematopoietic stem cell compartment and culture-induced stem cell impairment. Blood. 2004;103:545-552.
28. Nash R, Storb R, Neiman P. Polyclonal reconstitution of human marrow after allogeneic bone marrow transplantation. Blood. 1988;72:2031-2037.
29. Turhan AG, Humphries RK, Phillips GL, Eaves AC, Eaves CJ. Clonal hematopoiesis demonstrated by X-linked DNA polymorphisms after allogeneic bone marrow transplantation. N Engl J Med. 1989;320:1655-1661.
30. Brenner MK, Rill DR, Moen RC, et al. Gene-marking to trace origin of relapse after autologous bone-marrow transplantation. Lancet. 1993;341:85-86.
31. Dunbar CE, Cottler-Fox M, O'Shaughnessy JA, et al. Retrovirally marked CD34-enriched peripheral blood and bone marrow cells contribute to long-term engraftment after autologous transplantation. Blood. 1995;85:3048-3057.
32. Kohn DB, Weinberg KI, Nolta JA, et al. Engraftment of gene-modified umbilical cord blood cells in neonates with adenosine deaminase deficiency. Nat Med. 1995;1:1017-1023.
33. Schmidt M, Carbonaro DA, Speckmann C, et al. Clonality analysis after retroviral-mediated gene transfer to CD34+ cells from the cord blood of ADA-deficient SCID neonates. Nat Med. 2003;9:463-468.
34. Schmidt M, Hacein-Bey-Abina S, Wissler M, et al. Clonal evidence for the transduction of CD34+ cells with lymphomyeloid differentiation potential and self-renewal capacity in the SCID-X1 gene therapy trial. Blood. 2005;105:2699-2706.
35. Leonard WJ, Shores EW, Love PE. Role of the common cytokine receptor gamma chain in cytokine signaling and lymphoid development. Immunol Rev. 1995;148:97-114.
36. Miller JS, McCullar V, Punzel M, Lemischka IR, Moore KA. Single adult human CD34(+)/Lin-/CD38(+) progenitors give rise to natural killer cells, B-lineage cells, dendritic cells, and myeloid cells. Blood. 1999;93:96-106.
37. Robin C, Pflumio F, Vainchenker W, Coulombel L. Identification of lymphomyeloid primitive progenitor cells in fresh human cord blood and in the marrow of nonobese diabetic-severe combined immunodeficient (NOD-SCID) mice transplanted with human CD34(+) cord blood cells. J Exp Med. 1999;189:1601-1610.

38 Goldschneider I, Komschlies KL, Greiner DL. Studies of thymocytopoiesis in rats and mice. I: kinetics of appearance of thymocytes using a direct intrathymic adoptive transfer assay for thymocyte precursors. J Exp Med. 1986;163:1-17.

39 Allman D, Sambandam A, Kim S, et al. Thymopoiesis independent of common lymphoid progenitors. Nat Immunol. 2003;4:168-174.

40 Dick JE. Stem cells: self-renewal writ in blood. Nature. 2003;423:231-233.

41 Osawa M, Nakamura K, Nishi N, et al. In vivo self-renewal of c-Kit + Sca-1 + Lin(low/-) hemopoietic stem cells. J Immunol. 1996;156:3207-3214.

42 Pawliuk R, Eaves C, Humphries RK. Evidence of both ontogeny and transplant dose-regulated expansion of hematopoietic stem cells in vivo. Blood. 1996;88:2852-2858.

43 Holyoake TL, Nicolini FE, Eaves CJ. Functional differences between transplantable human hematopoietic stem cells from fetal liver, cord blood and adult marrow. Exp Hematol. 1999;27:1418-1427.

44 Cashman J, Dykstra B, Clark-Lewis I, Eaves A, Eaves C. Changes in the proliferative activity of human hematopoietic stem cells in NOD/SCID mice and enhancement of their transplantability after in vivo treatment with cell cycle inhibitors. J Exp Med. 2002;196:1141-1149.

45 Rosendaal M, Hodgson GS, Bradley TR. Organization of haemopoietic stem cells: the generation-age hypothesis. Cell Tissue Kinet. 1979;12:17-29.

46 Harrison DE, Astle CM. Loss of stem cell repopulating ability upon transplantation. Effects of donor age, cell number, and transplantation procedure. J Exp Med. 1982;156:1767-179.

47 Allsopp RC, Morin GB, Horner JW, DePinho R, Harley CB, Weissman IL. Effect of TERT overexpression on the long-term transplantation capacity of hematopoietic stem cells. Nat Med. 2003;9:369-371.

48 Ema H, Sudo K, Seita J, et al. Quantification of self-renewal capacity in single hematopoietic stem cells from normal and Ink-deficient mice. Dev Cell. 2005;8:907-914.

49 Bonnet D, Dick JE. Human acute myeloid leukemia is organized as a hierarchy that originates from a primitive hematopoietic cell. Nat Med. 1997;3:730-737.

50 Hope KJ, Jin L, Dick JE. Acute myeloid leukemia originates from a hierarchy of leukemic stem cell classes that differ in self-renewal capacity. Nat Immunol. 2004;5:738-743.

A novel nonpeptidyl human c-Mpl activator stimulates human megakaryopoiesis and thrombopoiesis

Takanori Nakamura, Yoshitaka Miyakawa, Atsushi Miyamura, Akiko Yamane, Hidenori Suzuki, Mamoru Ito, Yasuyuki Ohnishi, Norihisa Ishiwata, Yasuo Ikeda, and Nobutomo Tsuruzoe

NIP-004 is a novel synthetic compound developed to display human thrombopoietin (TPO) receptor (c-Mpl) agonist activity. NIP-004 displays species specificity, stimulating proliferation or differentiation of human c-Mpl–expressing cells such as UT-7/TPO and human CD34$^+$ cells but not murine c-Mpl–expressing cells or cynomolgus monkey cells. To test the mechanism of its action, we constructed mutant forms of c-Mpl; murine c-Mpl^{L490H} displayed a response to NIP-004, whereas human c-Mpl^{H499L} lost this response, indicating that histidine in the transmembrane domain of c-Mpl is essential for its activity. Because histidine is not present in the c-Mpl transmembrane domain of rats, hamsters, rhesus macaques, and cynomolgus monkeys, we examined the in vivo efficacy of NIP-004 using mice that received xenotransplants. In immunodeficient nonobese diabetic (NOD)/Shi-*scid*, IL-2Rγ^{null} (NOG) mice receiving transplants of umbilical cord blood–derived CD34$^+$ cells, NIP-004 increased human megakaryoblasts, mature megakaryocytes, and circulating human platelets 6-fold, the latter being morphologically and functionally indistinguishable from normal human platelets. These observations indicate that NIP-004 is a novel human c-Mpl activator and induces human thrombopoiesis. (Blood. 2006;107: 4300-4307)

Introduction

Platelets are important cells for preventing bleeding following injury. Thrombopoietin (TPO), a cytokine produced primarily by the liver and kidney, regulates platelet production by stimulating proliferation and differentiation of hematopoietic stem cells, megakaryocytic progenitor cells, and megakaryocytes via activation of its receptor, c-Mpl.[1-5] c-Mpl belongs to the type I cytokine receptor family, and like erythropoietin (EPO) and granulocyte colony-stimulating factor (GCSF) receptors, a major conformational change of the homodimeric receptor ensues upon TPO binding, followed by phosphorylation of the intracellular domain of c-Mpl and various secondary signaling molecules.[6] Among the signaling molecules activated by TPO are Janus kinases (Jaks) and signal transducers and activators of transcription (STATs), phosphatidylinositol-3-kinase (PI3K)/Akt, and Ras/mitogen-activated protein kinase (MAPK). Activation of these signaling pathways results in the induction of megakaryopoiesis and thrombopoiesis from hematopoietic stem cells.[6] Recombinant human (rh)TPO has been proven to be effective for the treatment of thrombocytopenia in some clinical settings.[7] However, adverse events of therapy have been reported, such as the development of neutralizing antibodies to TPO, followed by thrombocytopenia or pancytopenia.[8] A nonpeptidyl synthetic compound displaying c-Mpl agonistic activity would therefore offer important medical advantages for the treatment of thrombocytopenia.

Toward this end, we developed a novel human c-Mpl (HuMpl) agonist, NIP-004, that displays species specificity. While NIP-004 stimulated HuMpl-expressing cells such as human bone marrow (BM)–, peripheral blood (PB)–, and umbilical cord blood (CB)–derived CD34$^+$ cells, it did not induce proliferation of murine c-Mpl (MuMpl)–expressing cells or colony formation of megakaryocytes with BM cells from murine or cynomolgus monkey. Using mutants of the c-Mpl receptor, we also found that substitution of histidine (His) for leucine (Leu) (L490H) in the MuMpl transmembrane domain allowed the murine receptor to respond to NIP-004. Conversely, HuMpl^{H499L} lost its response to NIP-004, indicating that the His residue is essential for NIP-004 activity. Because this His residue is only present in the HuMpl transmembrane domain, this observation also helps to explain the species specificity of NIP-004. Moreover, this property requires a xenotransplantation model to evaluate the in vivo biologic activities of NIP-004. We used immunodeficient nonobese diabetic (NOD)/Shi-*scid*, IL-2Rγ^{null} (NOG) mice as recipients. These mice exhibit highly potent reconstitutive activity for human hematopoietic stem cells and can maintain human hematopoiesis,[9] including megakaryopoiesis and thrombopoiesis, for at least 6 months after transplantation (Y.M.,

From the Pharmaceutical Research Department, Biological Research Laboratories, Nissan Chemical Industries, Saitama; Department of Internal Medicine, Keio University School of Medicine, Tokyo; Medical Research & Development Center, Tokyo Metropolitan Institute of Medical Science, Tokyo; and Central Institute for Experimental Animals, Kanagawa, Japan.

Submitted November 10, 2005; accepted January 21, 2006. Prepublished online as *Blood* First Edition Paper, February 16, 2006; DOI 10.1182/blood-2005-11-4433.

Several of the authors (T.N., A.M., N.I., and N.T.) are employed by a company (Nissan Chemical Industries) whose product was studied in the present work.

T.N., Y.M., and N.I. designed the study; T.N., A.M., A.Y., and H.S. carried out the research; M.I. and Y.O. contributed live mice; T.N., Y.M., A.M., and H.S. analyzed the data; N.I., Y.I., and N.T. controlled the data; T.N. and Y.M. wrote the paper; and all authors checked the final version of the manuscript.

Reprints: Takanori Nakamura, Pharmaceutical Research Department, Biological Research Laboratories, Nissan Chemical Industries, Ltd, 1470 Shiraoka, Saitama 349-0294, Japan; e-mail: tnakamura@nissanchem.co.jp.

The publication costs of this article were defrayed in part by page charge payment. Therefore, and solely to indicate this fact, this article is hereby marked "advertisement" in accordance with 18 U.S.C. section 1734.

T.N., Hiroshi Yoshida, M.I., Y.O., and Y.I., manuscript in preparation). Using this model, we demonstrated that NIP-004 possesses HuMpl agonistic activity in vivo, and these data support the in vitro activity of the molecule.

Materials and methods

Reagents

Our search for c-Mpl activators was based on proliferation assays using TPO-responsive cell lines with our chemical library (Nissan Chemical Industries, Chiba, Japan), which comprises approximately 50 000 compounds. This process resulted in the identification of several compounds displaying growth-promoting activities. Lead optimization was performed based on the conversion of scaffold and functional groups to increase the growth-promoting activity of the lead compound. Finally, a novel nonpeptidyl HuMpl activator, NIP-004 (5-[(2-{1-[5-(3,4-dichlorophenyl)-4-hydroxy-3-thienyl]ethylidene}hydrazino)carbonyl]-2-thiophenecarboxylic acid) was chemically constructed at Nissan Chemical Industries. We also synthesized another human TPO mimetic, SB-497115. Its structure was presented in a poster presentation at the 46th annual meeting of the American Society of Hematology.[10] Cytokines including rhTPO (PeproTech, Rocky Hill, NJ, and R&D Systems, Minneapolis, MN), rhEPO (Chugai Pharmaceutical, Tokyo, Japan), recombinant murine (rm) interleukin-3 (IL-3) (R&D Systems), rhIL-3 (R&D Systems), and rhGCSF (PeproTech) were obtained as indicated.

Cells

Cells used in this study were human myeloblastic leukemia cell lines UT-7, UT-7/TPO, and UT-7/EPO (kindly donated by Dr Norio Komatsu, University of Yamanashi, Japan), murine pro–B-cell line Ba/F3 (Riken Cell Bank, Tsukuba, Japan), and human embryonic kidney cell line HEK293 (Health Science Research Resources Bank, Osaka, Japan). UT-7/EPO-HuMpl in which the human *c-mpl* gene was genetically introduced under the control of cytomegalovirus (CMV) promoter was kindly donated by Dr Norio Komatsu. Stable transfectants such as UT-7/EPO-MuMpl, Ba/F3-HuMpl, Ba/F3-MuMpl, and Ba/F3-HuGCSFR were established to transfect human or murine *c-mpl* or human *gcsfr* genes under the control of the CMV promoter (pcDNA3 vector; Invitrogen, Carlsbad, CA) using electroporation. UT-7 cells and the variant cell lines were maintained in Iscove modified Dulbecco medium (IMDM) supplemented with 10% fetal bovine serum (FBS) and rhIL-3, rhTPO, or rhEPO. Ba/F3 cells and their transfectants were maintained in RPMI 1640 medium supplemented with 10% FBS and rmIL-3, rhTPO, or rhGCSF. HEK293 cells were cultured in Dulbecco modified Eagle medium (DMEM) containing 10% FBS. Human primary hematopoietic progenitor cells were BM-, PB-, or CB-derived CD34$^+$ cells (Cambrex, East Rutherford, NJ). Cynomolgus BM-derived CD34$^+$ cells were prepared from BM mononuclear cells (Cambrex) using a CD34 progenitor cell selection system (Dynabeads M-450 CD34; Dynal Biotech, Oslo, Norway). Murine BM cells were prepared from BALB/c mice (Japan SLC, Shizuoka, Japan).

Genes

The cDNAs of human or murine *c-mpl* or human *gcsfr* were amplified by reverse transcriptase–polymerase chain reaction (RT-PCR) using a SuperScript First-Strand Synthesis System (Invitrogen) and each specific primer set as follows: human *c-mpl* primer set (sense, 5′-ATGCCCTCCTGGGCCCTCTT-3′; antisense, 5′-TCAAGGCTGCTGCCAATAGCT-3′), murine *c-mpl* primer set (sense, 5′-ATGCCCTCTTGGGCCCTCTTCAT-3′; antisense, 5′-TCAGGGCTGCTGCCAATAGCTTAGT-3′), and human *gcsfr* primer set (sense, 5′-ATGGCAAGGGCTGGGAAACTGCA-3′; antisense, 5′-CTAGAAGCTCCCCAGCGCCTCCA-3′). Full-length cDNAs were cloned into pCR vector (Invitrogen) and were subcloned into the *Eco*RI site of the pcDNA3 vector. In vitro mutagenesis of human or murine *c-mpl* genes (HuMpl^{W490L} or MuMpl^{L456H}) was performed using QuikChange Site-Directed Mutagenesis Kit (Stratagene, La Jolla, CA) and a specific primer set as follows: HuMpl^{W490L} primer set (sense, 5′-GGTGACCGCTCTGCTACTAGTGCTGGGCC-3′; antisense, 5′-GGCCCAGCACTAGTAGCAGAGCGGTCACC-3′) and MuMpl^{L456H} primer set (sense, 5′-GTGACTGCTCTGCACCTGGTGCTGAGC-3′; antisense, 5′-GCTCAGCACCAGGTGCAGAGCAGTCAC-3′), according to the protocols of the manufacturer. The cDNAs of cynomolgus monkey, rhesus macaque, common marmoset, and squirrel monkey *c-mpl* homologous genes were amplified by RT-PCR using a human *c-mpl* primer set and total RNA isolated from whole blood for each nonhuman primate (Hamri, Ibaraki, Japan). A human *c-mpl* primer set and a nested primer set (sense, 5′-CTTTGGAACCCGATACGTGTG-3′; antisense, 5′-GGAGGATTTCCAGGAGGCTG-3′), designed for high-sequence homology between human and murine *c-mpl* genes, were used for amplification in Japanese white rabbit (Kitayama Labes, Nagano, Japan), Syrian hamster, Hartley guinea pig (Japan SLC), and Wistar rat (Charles River Japan, Kanagawa, Japan) *c-mpl* homologous genes. The cDNAs of these animal *c-mpl* homologous genes were cloned into the pCR vector, and their sequences were identified as accession numbers AB235193, AB235192, AB235194, AB235195, AB235199, AB235198, AB235196, and AB235197 for cynomolgus monkey, rhesus macaque, common marmoset, squirrel monkey, Japanese white rabbit, Syrian hamster, Hartley guinea pig, and Wistar rat, respectively.

Proliferation assay

A total of 2×10^3 to 6×10^3 cells were harvested in IMDM or RPMI 1640 medium containing 10% FBS and cytokines or NIP-004 at the indicated final concentration and incubated in a CO_2 incubator (5% CO_2, 37°C) for 3 to 4 days, depending on the cell line. Cell proliferation was assayed using WST-8 reagent (Kishida Chemical, Osaka, Japan) according to instructions from the manufacturer. The formazan pigment was detected by measuring absorbance at 450 nm with a 96-well microplate reader, Spectramax 190 (Molecular Devices, Sunnyvale, CA) or Model 550 (Bio-Rad, Hercules, CA).

Immunoprecipitation and Western blotting

A total of 2×10^7 UT-7/EPO-HuMpl cells were starved for 17 hours at 37°C and stimulated with 20 μg/mL NIP-004 or 30 ng/mL hTPO at 37°C for 15 minutes. Cells were solubilized in 1 mL TNE buffer comprising 20 mM Tris-HCl buffer (pH 7.4), 150 mM NaCl, 1 mM ethylenediaminetetraacetic acid (EDTA), 1% Triton X-100, 1 mM phenyl methane sulfonyl fluoride, 1 mM Na_3VO_4, and 1:400-diluted protease inhibitor cocktail (Sigma, St Louis, MO). After centrifugation, cleared lysates were incubated with anti-Mpl (IBL, Gunma, Japan), anti-Jak2 (Upstate Biotechnology, Waltham, MA), and anti-STAT5a (Upstate Biotechnology) for 1 hour at 4°C. Immune complexes adsorbed with protein G–Sepharose were resolved by 7.5% sodium dodecyl sulfate–polyacrylamide gel electrophoresis. Transferred polyvinylidene fluoride membrane (Millipore, Bedford, MA) was immunoblotted with monoclonal antiphosphotyrosine antibody (BD PharMingen, San Diego, CA) or anti-Mpl, anti-Jak2, or anti-STAT5a and alkaline phosphatase (AP)–labeled secondary antibody (Invitrogen); then the proteins were visualized using nitroblue tetrazolium and 5-bromo-4-chloro-3-indolyl phosphate reagents (Bio-Rad).

Megakaryocyte colony-forming unit assay

Megakaryocyte colony-forming unit (CFU-MK) assays were performed using MegaCult-C (StemCell, Vancouver, BC, Canada) according to the manufacturer's protocol. A total of 7.5×10^3 human or cynomolgus monkey BM-derived CD34$^+$ cells or 2.5×10^3 human CB- or PB-derived CD34$^+$ cells were cultured with NIP-004 or rhTPO for 11 days in collagen-based, semisolid medium. After fixation, megakaryocytes were visualized with antibody against CD41a using AP staining. Nuclei were stained with Evans blue. Stained colonies were examined under a Nikon Eclipse E800 microscope equipped with a 10 × 0.3 numeric aperture (NA) objective lens (Nikon, Tokyo, Japan). Images were captured using an Olympus Camedia C300 digital camera (Olympus, Tokyo, Japan). The murine CFU-MK assay was performed as follows: 3×10^5 murine BM cells were cultured with NIP-004 or rhTPO for 7 days in agar-based, semisolid medium comprising IMDM, 1% bovine

serum albumin, 0.6 mg/ml transferrin, 8 μg/ml cholesterol, and 0.4% agar. After fixation in glutaraldehyde, megakaryocytes were visualized by measuring the internal acetyl cholinesterase activity as previously described.[11]

Luciferase assay

HEK293 cells were transfected with pcDNA-HuMpl, HuMpl$^{[1-491]}$, MuMpl, or MuMpl$^{[1-490]}$ in combination with pXM-MGF (STAT5) and acute phase response element–luciferase construct (kindly donated by Dr Akihiko Yoshimura[12]) using the Effectene transfection reagent (Qiagen, Hilden, Germany). Twenty-four hours after transfection, cells were starved for 8 hours, followed by stimulation with rhTPO or NIP-004 at the indicated concentration for 18 hours. Cell extracts were prepared, and luciferase activity was measured using PicaGene reagent (Toyo B-NET, Tokyo, Japan) according to the manufacturer's instructions.

Xenotransplantation assay

NOG mice were developed at the Central Institute for Experimental Animals (Kanagawa, Japan) and were maintained under specific pathogen-free conditions. Shortly before cell transfer, 8- to 10-week-old NOG mice were irradiated with 2.4 Gy x-rays. Frozen 1×10^5 CB-derived CD34$^+$ cells were washed with IMDM medium supplemented with 0.1% BSA and the cells then intravenously inoculated into mice. After transplantation, mice were provided with sterile water containing prophylactic neomycin sulfate (Gibco BRL, Grand Island, NY). Mice received daily subcutaneous administration of NIP-004 for the indicated period at a dosage of 10 or 30 mg/kg (with PBS containing 1.6% PEG400 and 2.4% ethanol vehicle) from 2 to 6 months after transplantation. Whole blood containing EDTA-2Na or 0.38% sodium citrate was prepared recurrently from a mouse. Complete blood counts were obtained using a K-4500 automated analyzer (Sysmex, Hyogo, Japan). BM cells were obtained by flushing the femurs, and cell numbers were counted using a hemocytometer (Erma, Tokyo, Japan) after staining with Turk solution.

Flow cytometry analysis

To detect human cells in murine blood, multicolor flow cytometry was performed using an EPICS-XL flow cytometer (Beckman Coulter, Franklin Lakes, NJ). Samples were incubated with the indicated antibodies for 30 minutes at 4°C and were depleted of erythrocytes by fixation in fluorescence-activated cell sorter (FACS) lysing solution (BD PharMingen). Antibodies used in this study were as follows: anti–human CD33–fluorescein isothiocyanate (FITC), CD3-FITC, CD41a-FITC, CD34-FITC, CD71-FITC, CD34-phycoerythrin (PE), CD41a-PE, CD19-PE, CD45-PE Texas red (ECD), CD38-PE 5-succinimidylester (PC5), anti–murine CD45-FITC, and CD41-FITC. Antibodies conjugated with FITC, PE, or PC5 were purchased from BD PharMingen. Antibodies conjugated with ECD were purchased from Immunotech (Marseilles, France). Platelets were incubated with the indicated antibodies at room temperature and directly applied to the flow cytometer. Human platelets were examined by double staining with anti–murine CD41-FITC antibody and anti–human CD41a-PE antibody, in which platelets were identified by size and gated by forward and side scatter. The actual number of human CD41a$^+$ platelets was calculated as follows: actual human CD41a$^+$ platelet count = (human CD41a$^+$ platelet count/[human CD41a$^+$ platelet count + murine CD41$^+$ platelet count]) × whole platelet count.

To detect human megakaryocyte ploidy, BM cells from NOG mice that received xenotransplants were stained using anti–human CD41a-PE antibody and fixed with 1% paraformaldehyde. Fixed cells were stained using 7-amino-actinomycin D (7-AAD) dye (Immunotech) and examined by 2-color cytometric analysis.

Immunohistochemistry

Femurs of NOG mice that received xenotransplants were removed for histologic examination. Tissue was fixed in neutral buffered formalin and decalcified, followed by paraffin embedding and sectioning. Immunohistochemistry was performed with murine monoclonal antibodies against human CD42b (Chemicon, Temecula, CA) and EnVision+ peroxidase staining kit (Dako, Carpinteria, CA). Stained sections were examined using an Olympus BX51 microscope equipped with a 10 × 0.3 NA objective and connected to an Olympus DP12 camera, using DP12 software.

Electron microscopic analysis of human platelets from mice undergoing xenotransplantation

Immunoelectron microscopy was performed as previously described.[13] Whole blood containing 0.38% sodium citrate, 1 μM prostaglandin E_1, 2 U/ml apyrase, and 2 mM aspirin (Sigma) was prepared. Platelet-rich plasma (PRP) was fixed with glutaraldehyde and sequentially immersed in 1 M sucrose, 1.84 M sucrose, and 1.84 M sucrose with 20% polyvinylpyrrolidone (MW 10 000; Sigma) in PBS. After freezing platelets in liquid nitrogen, ultrathin frozen sections were cut using an Ultracut ultramicrotome (Reichert, Vienna, Austria) with a cryoattachment (FC-4E; Reichert) at −90°C. Sections were mounted on nickel grids and incubated with anti–human CD41a monoclonal antibody (Immunotech), followed by goat anti–mouse IgG coupled to colloidal gold (10 nm; Amersham, Olen, Belgium). Sections were stained with uranyl acetate and subjected to adsorption staining using a mixture of polyvinyl alcohol and uranyl acetate. Stained sections were examined using a JEM 1200EX electron microscope (JEOL, Tokyo, Japan) at an accelerating voltage of 80 kV.

Functional studies of platelets from NOG mice undergoing xenotransplantation

Functional studies of platelets were performed as previously described.[14] After administration of NIP-004 (30 mg/kg/d subcutaneously for 14 days) or vehicle, PRP was obtained, and *N*-2-hydroxyethylpiperazine-*N*′-2-ethanesulfonic acid (HEPES)–Tyrode buffer (138 mM NaCl, 0.42 mM NaH_2PO_4, 2.68 mM KCl, 12 mM $NaHCO_3$, 10 mM HEPES, 5 mM glucose, and 1.7 mM $MgCl_2$, pH 7.4) was added at a 1:9 ratio. To determine the expression of P selectin upon agonist stimulation, platelets were stimulated using 10 μM ADP or vehicle for 15 minutes in the buffer containing anti–human CD62p-PE antibody (BD PharMingen). After fixation with 0.5% paraformaldehyde, cells were washed and incubated with anti–human CD41a-PC5 (BD PharMingen) and anti–murine CD41-FITC antibody. To determine the activation of GPIIb-IIIa, platelets were stimulated with 0 to 10 μM ADP for 15 minutes with PAC-1–FITC (BD Pharmingen), anti–human CD42b-PC5, and anti–murine CD61-PE antibody and then fixed and washed. Stained platelets were analyzed by flow cytometry.

Statistical analysis and ethical considerations

Results are expressed as mean ± SD or mean ± SEM as indicated. Differences between groups were examined for statistical significance using the Student *t* test. Animal experiments were conducted according to the "Guideline for animal experimentation"[15] by the Japanese Association for Laboratory Animal Science. All experimental protocols were approved by the ethics review committees for animal experimentation of Keio University and Nissan Chemical Industries.

Results

NIP-004 is a novel human c-Mpl activator

We conducted a search for c-Mpl activators based on proliferation assays with TPO-responsive UT-7/TPO and UT-7/EPO-HuMpl cell lines. Screened agents were obtained from our chemical library, comprising approximately 50 000 compounds. This process resulted in the identification of several compounds displaying growth-promoting activity. Lead optimization was subsequently performed to create c-Mpl activators with greater growth-promoting activity. NIP-004 is a synthetic compound (MW 455; Figure 1A) and stimulated the proliferation of UT-7/TPO,[16] a human leukemia cell line endogenously expressing HuMpl, in a

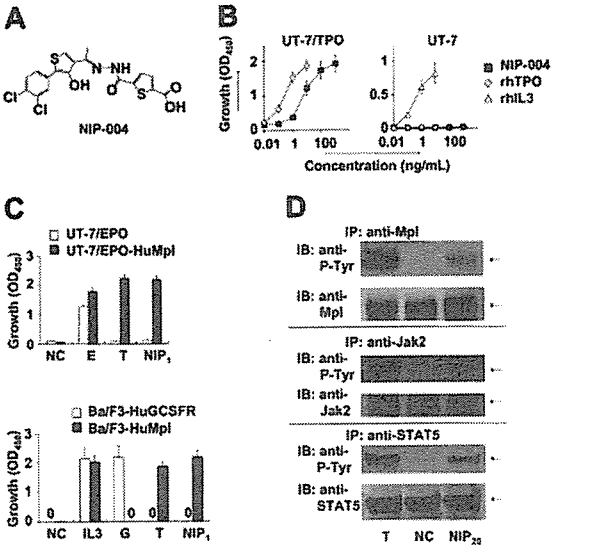

Figure 1. NIP-004 is a novel human c-Mpl activator. (A) Chemical structure of NIP-004. (B) Dose-dependent proliferation of UT-7/TPO cells, but not parental UT-7 cells, by NIP-004. Recombinant human TPO and rhIL-3 induced proliferation of UT-7/TPO and parental UT-7 cells, respectively. (C) TPO and NIP-004 induced proliferation of UT-7/EPO-HuMpl but not UT-7/EPO (top panel). EPO stimulated proliferation of UT-7/EPO and UT-7/EPO-HuMpl as a positive control. NIP-004 stimulated proliferation of Ba/F3-HuMpl but not Ba/F3-HuGCSFR (bottom panel). GCSF stimulated Ba/F3-HuGCSFR cells. TPO induced proliferation of Ba/F3-HuMpl cells as a positive control. IL-3 stimulated both Ba/F3-HuGCSFR and Ba/F3-HuMpl. Data in panels B-C are expressed as the mean ± SEM (n = 3 to 4) or mean ± SD (n = 2; Ba/F3-HuGCSFR) from independent duplicate experiments. (D) Induction of tyrosine phosphorylation of c-Mpl, Jak2, and STAT5 in UT-7/EPO-HuMpl cells by TPO and NIP-004. NC indicates negative control; E, 0.1 U/mL rhEPO; IL-3, 0.1 ng/mL rmIL-3; G, 10 ng/mL rhGCSF; T, 10 ng/mL rhTPO; NIP_1, 1 μg/mL NIP-004; NIP_{20}, 20 μg/mL NIP-004; P-Tyr, phosphotyrosine.

dose-dependent manner (Figure 1B). Compared with 10 ng/mL rhTPO, which induces a maximal response in this cell line, the median effective concentration (EC_{50}) of NIP-004 was 23 ng/mL (50 nM) in UT-7/TPO cells (Figure 1B). Proliferation of UT-7 cells, the parental cell line of UT-7/TPO, can be induced by cytokines such as human IL-3, human granulocyte-macrophage colony-stimulating factor (GMCSF), IL-6, stem cell factor, and EPO but not by TPO because UT-7 does not display c-Mpl.[16,17] Consistent with its action through c-Mpl, NIP-004 did not induce the growth of UT-7 cells (Figure 1B, right panel). Recombinant human IL-3 induced proliferation of UT-7 cells as a positive control. We also confirmed the roles of HuMpl using other cell lines as follows. When HuMpl was introduced into UT-7/EPO cells,[18,19] UT-7/EPO-HuMpl transfectants responded to both rhTPO and NIP-004 (Figure 1C, upper panel). NIP-004 induced proliferation of Ba/F3-HuMpl cells but not Ba/F3-HuGCSFR cells expressing human GCSF receptor, indicating that NIP-004 acts on c-Mpl (Figure 1C, lower panel). Recombinant human GCSF and rhTPO stimulated proliferation of Ba/F3-HuGCSFR and Ba/F3-HuMpl cells as positive controls, respectively (Figure 1C).

A large body of evidence indicates that like other type I family cytokine receptors, TPO signaling is dependent on Jak-induced phosphorylation of tyrosine residues within the cytoplasmic domain of c-Mpl. Subsequently, secondary signaling molecules, including STAT5, are recruited to the phosphotyrosine residues and are activated by their phosphorylation.[1] Administration of 20 μg/mL NIP-004 induced phosphorylation of c-Mpl, Jak2, and STAT5 proteins in UT-7/EPO-HuMpl cells after 15 minutes (Figure 1D). TPO was used as positive control stimulation (Figure 1D). In addition, rhTPO and NIP-004 induced phosphorylation of Akt, an antiapoptotic protein in the PI3K-Akt signaling pathway, via c-Mpl (data not shown).

We next examined whether NIP-004 possessed the capacity to induce megakaryocyte differentiation using colony-forming assays and histologic staining with a monoclonal antibody against integrin GPIIb-IIIa (CD41a), a specific marker of the megakaryocyte-platelet lineage.[20] NIP-004 1 μg/mL alone stimulated colony formation of $CD41a^+$ megakaryocytes from human BM-derived $CD34^+$ hematopoietic progenitor cells in serumfree, semisolid cultures (Figure 2A). NIP-004 induced maturation of megakaryocytes, since large polyploid $CD41a^+$ cells appeared in the colony (Figure 2A). NIP-004 increased the number of CFU-MKs from human BM-derived $CD34^+$ cells in a dose-dependent manner (Figure 2B, left panel). Furthermore, a number of CFU-MKs developed from human CB- or PB-derived $CD34^+$ cells treated with NIP-004 (Figure 2B). The efficiency of CFU-MK production in $CD34^+$ cells was higher in CB- and PB-derived cells than in BM-derived cells, as previously reported (Figure 2B, right panel).[21]

NIP-004 displays species-specific activity

Because NIP-004 was obtained using cells expressing HuMpl, the effects of NIP-004 on c-Mpl from other species were examined. NIP-004 did not induce proliferation of UT-7/EPO-MuMpl or Ba/F3-MuMpl cells, which were engineered to express murine c-Mpl receptor (Figure 3A). Furthermore, NIP-004 did not increase the number of CFU-MK colonies from murine BM cells or cynomolgus monkey BM-derived $CD34^+$ cells within the effective dosage for human cells (Figure 3B). Likewise, rhesus macaque BM-derived $CD34^+$ cells failed to form CFU-MK colonies in the presence of a NIP-004–derived compound (data not shown). These results indicate that NIP-004 displays species specificity.

To identify the molecular basis for the species specificity displayed by NIP-004, we analyzed the amino acid sequence of c-Mpl from 2 nonhuman primates, cynomolgus and rhesus monkeys, and compared them with the HuMpl and MuMpl. Cynomolgus c-Mpl displayed the highest level of sequence homology, 96%

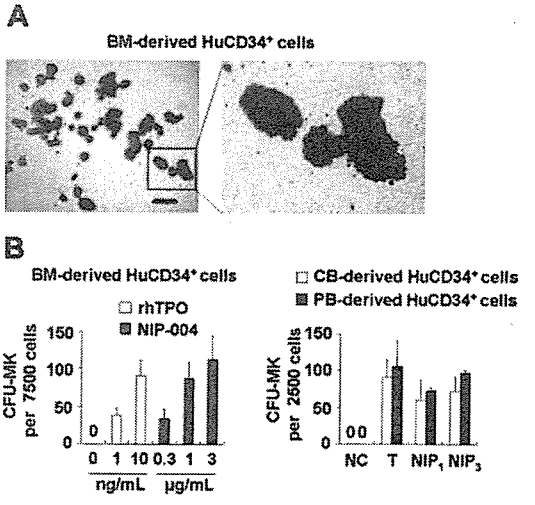

Figure 2. Stimulation of megakaryocyte colony formation from human $CD34^+$ cells by NIP-004. (A) Morphology of CFU-MK colonies obtained from human BM-derived $CD34^+$ cells treated with 1 μg/mL NIP-004. CFU-MKs were visualized with AP-labeled antibody against human CD41. Polyploid megakaryocytes are shown in detail in the right panel. Bar, 200 μm. (B) The number of CFU-MKs from human BM-, CB-, and PB-derived $CD34^+$ cells treated with 1 to 3 μg/mL NIP-004 was similar to that with 10 ng/mL rhTPO. Results are expressed as mean ± SEM from 4 independent experiments (BM) or mean ± SD from 2 independent experiments (CB and PB). NC indicates negative control; T, 10 ng/mL rhTPO; NIP_1, 1 μg/mL NIP-004; NIP_3, 3 μg/mL NIP-004.

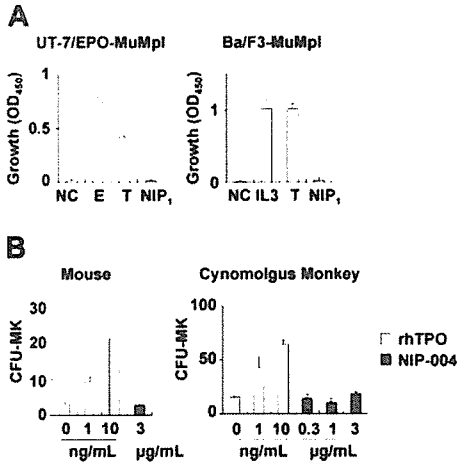

Figure 3. NIP-004 displays species-specific activity. (A) NIP-004 failed to stimulate proliferation of UT-7/EPO-MuMpl– and Ba/F3-MuMpl–expressing murine Mpl. In contrast, EPO and TPO stimulated induced proliferation of UT-7/EPO-MuMpl as a positive control. IL-3 and TPO enhanced proliferation of Ba/F3 MuMpl as a positive control. Data are expressed as the mean ± SEM from 3 independent experiments. (B) Recombinant human TPO stimulated CFU-MK colony formation from murine and cynomolgus monkey–derived bone marrow cells in a dose-dependent manner. In contrast, NIP-004 failed to induce CFU-MK colonies under the same conditions. Data are expressed as the mean ± SD of duplicate assays. NC indicates negative control; E, 0.1 U/mL rhEPO; IL-3, 0.1 ng/mL rmIL-3; T, 10 ng/mL rhTPO; NIP1, 1 µg/mL NIP-004

identical to HuMpl, with only 22 amino acids differing between the 2 species, and 12 of the 22 amino acids of HuMpl differed from rhesus c-Mpl. Comparison of these 12 amino acid residues as either hydrophobic or hydrophilic, and either electrically charged or uncharged, revealed distinguishing features of the amino acid residues. His at position 499 from the N-terminal end in the transmembrane domain of HuMpl is specific for humans. We thus performed site-directed mutagenesis for this residue in HuMpl and MuMpl (Figure 4A) and analyzed STAT5 activation via each receptor in the HEK293 cell line using the STAT-reporter gene assay (Figure 4B). Wild-type HuMpl, but not MuMpl, activated STAT5 after stimulation with NIP-004 in a dose-dependent manner. HuMpl with His499 mutated to Leu failed to induce STAT5 activation following stimulation with NIP-004, although rhTPO was active. Conversely, when MuMpl was engineered to contain His490, as is present in the human receptor, it was then capable of activating STAT5 (Figure 4B). These observations indicate that His in the transmembrane domain of c-Mpl is essential for NIP-004 to function as a c-Mpl activator. We therefore assessed the c-Mpl amino acid sequence in several common experimental animals to find a suitable species in which we could evaluate the in vivo efficacy of NIP-004 for platelet production. Our search revealed no animals with His in the transmembrane domain of c-Mpl among the common marmoset, squirrel monkey, Japanese white rabbit, Syrian hamster, Hartley guinea pig, and Wistar rat (Figure 4C).

NIP-004 stimulates human megakaryopoiesis in NOG mice undergoing xenotransplantation

Because we were unable to find suitable experimental animals with His in the c-Mpl transmembrane domain to evaluate the effects of NIP-004, we selected a xenotransplantation model to examine in vivo efficacy of the compound for human megakaryopoiesis and thrombopoiesis. We used NOG mice to develop this new experimental animal model of human megakaryopoiesis, because this species displayed high potency for reconstituting human hematopoietic progenitor cells.[9]

In NOG mice receiving transplants with human CB-derived $CD34^+$ cells, treatment with 30 mg/kg/d NIP-004 for 2 weeks resulted in a 3-fold increase in human (Hu) $CD41a^+$ megakaryocytes in murine BM (0.9% in NIP-004–treated mice versus 0.3% in vehicle-treated mice) but no alteration in the number of murine $CD41^+$ megakaryocytes (Figure 5A). This dosage of NIP-004 achieved a plasma concentration of approximately 0.6 µg/mL at steady state. NIP-004 thus enhanced human megakaryopoiesis at an in vivo dosage comparable to that in the in vitro colony formation study (Figure 2B).

NIP-004 did not influence the total number of nucleated cells, the percentage of human or murine $CD45^+$ leukocytes, the percentage of $HuCD38^+CD19^+$ B lymphoid or $HuCD38^{low/-}CD33^+$ myeloid cells in $HuCD45^+$ cells, or the number of $HuCD45^-CD71^+$ erythroblasts in murine BM (Figure 5B). Although the total percentage of $HuCD45^+CD34^+$ hematopoietic progenitor cells was not altered by NIP-004 administration, we observed a 1.5-fold increase in the percentage of $HuCD45^+CD34^+CD41a^+$ megakaryoblasts (Figure 5C). This finding indicates that NIP-004 enhanced the number of human megakaryoblasts and megakaryocytes in xenotransplanted murine BM.

We next examined whether NIP-004 induced the maturation of megakaryocytes in vivo. DNA ploidy of $HuCD41^+$ megakaryocytes was analyzed by flow cytometry using anti-HuCD41 antibody and 7-AAD dye. In mice that received transplants, BM cells were prepared after treatment with NIP-004 (30 mg/kg/d for 2 weeks) or vehicle. Each ploidy class of human megakaryocytes was increased in mice treated with NIP-004, with statistical significance in all but the 32N class (Figure 5D). NIP-004 increased the percentage of $HuCD41a^+$ 128N megakaryocytes by a mean 2.7 ± 0.1 times.

Similar results were obtained in immunohistochemistry. BM from mice receiving xenotransplants was stained with monoclonal antibodies against human integrin GPIb (HuCD42b) to specifically visualize human megakaryocytes (Figure 5E-F). Murine megakaryocytes were not stained with this antibody. NIP-004 (30 mg/kg/d for

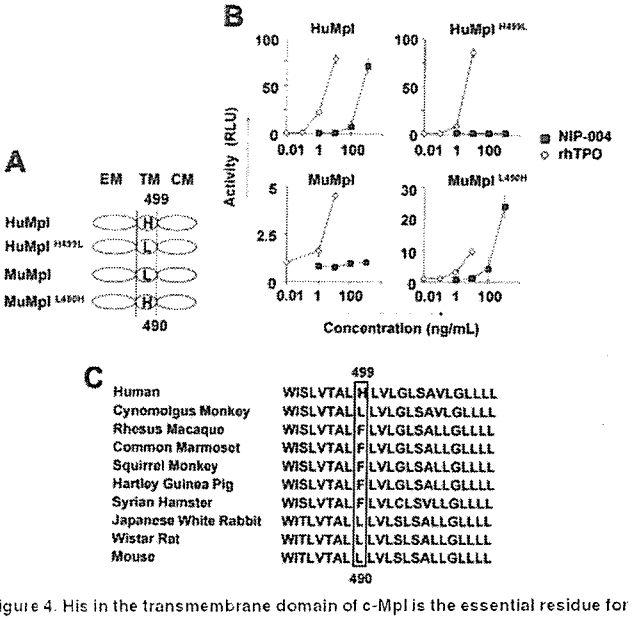

Figure 4. His in the transmembrane domain of c-Mpl is the essential residue for NIP-004. (A) Schema of site-directed mutagenesis in HuMpl and MuMpl. EM indicates extracellular module; TM, transmembrane module; CM, cytoplasmic module. (B) STAT5 reporter gene assay showing induction of STAT activation via HuMpl and $MuMpl^{L490H}$ but not $HuMpl^{H499L}$ or MuMpl following NIP-004 administration. Data are expressed as the mean ± SD from 2 independent experiments. (C) Comparison of amino acid sequences of c-Mpl transmembrane domain from various animals. His499 only exists in humans and not in other species.

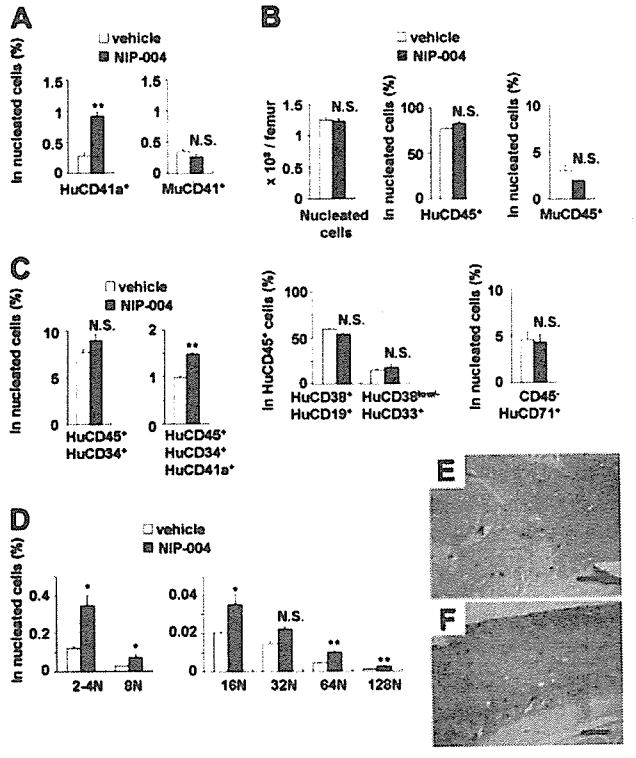

Figure 5. Effects of NIP-004 on human megakaryopoiesis in xenotransplanted murine bone marrow. (A) NIP-004 increased HuCD41a$^+$ megakaryocytes, but not MuCD41$^+$ megakaryocytes, in NOG mice receiving xenotransplants. (B) NIP-004 had no significant effect on the number of total nucleated cells and the percentage of other cell lines in murine BM. (C) NIP-004 increased the number of human megakaryocytic progenitor cells (HuCD45$^+$CD34$^+$CD41a$^+$) but not HuCD45$^+$CD34$^+$ hematopoietic progenitor cells. (D) FACS analysis of DNA ploidy of HuCD41$^+$ megakaryocytes. NIP-004 induced maturation of human megakaryocytes in the BM of NOG mice receiving xenotransplants. Data in panels A-D are expressed as mean ± SEM (n = 3). $^*P < .05$, $^{**}P < .01$ between NIP-004 and vehicle. N.S. indicates no significant difference compared with vehicle. Similar results were obtained from 2 independent experiments. (E-F) Immunohistochemical staining of xenotransplanted murine BM with a monoclonal antibody against human integrin GPIb (HuCD42b). Sections were obtained from the femurs of mice treated with vehicle (E) or NIP-004 (F). Bars, 200 μm.

2 weeks) clearly enhanced human megakaryopoiesis (Figure 5E-F). These findings demonstrate that NIP-004 specifically enhanced human megakaryopoiesis but not other types of human hematopoiesis in mice receiving xenotransplants.

NIP-004–induced production of human platelets in mice undergoing xenotransplantation

All NOG mice (n = 84) receiving transplants with human hematopoietic cells produced human platelets for at least 1 to 6 months. To clarify whether NIP-004 increased circulating human platelets in mice receiving xenotransplants, several administration protocols were used. NIP-004 30 mg/kg/d subcutaneously for 2 weeks induced a statistically significant 4.4-fold increase in circulating human CD41a$^+$ platelets at day 14 (Figure 6A). NIP-004 did not influence the total number (human and murine) of red blood cells, platelets, and white blood cells (Figure 6B, upper panel). The number of murine CD41$^+$ platelets and chimerisms of HuCD45$^+$ leukocytes was not altered by NIP-004 administration (Figure 6B, middle panel). Furthermore, NIP-004 did not influence the percentage of HuCD19$^+$ B lymphoid, HuCD3$^+$ T lymphoid, or HuCD33$^+$ myeloid cells among the circulating HuCD45$^+$ cells in mice receiving xenotransplants (Figure 6B, lower panel).

Next, the effect of the administration period or dosage was examined. When NOG mice receiving transplants with HuCD34$^+$ cells were treated with NIP-004 30 mg/kg/d for 5 weeks, there was a 6.4-fold increase in human platelets (Figure 6C). In mice receiving transplants, treatment with 10 mg/kg/d NIP-004 for 2 weeks resulted in a 3.2-fold increase in human platelets (Figure 6C). Human platelet counts returned to pretreatment levels after cessation of drug treatment (Figure 6C). When mice were reexposed to NIP-004, the number of human platelets increased again, suggesting human megakaryopoiesis was maintained in NOG mice undergoing xenotransplantation (data not shown).

To elucidate whether the human platelets in NIP-004–treated mice displayed normal morphologic features, immunoelectron microscopic analysis was performed using antibodies against HuCD41 and MuCD41. Platelets were prepared from mice after administration of NIP-004 30 mg/kg/d subcutaneously for 2 weeks, when human platelet chimerism increased from 2% at baseline to approximately 9%. Human platelets were labeled with gold particles to visualize HuCD41 (Figure 7A). Human platelets labeled with gold particles were larger than unlabeled murine platelets. Human platelets exhibited discoid forms similar to normal human peripheral platelets,[13] containing some granules, mitochondria, and other organelles. Conversely, when antibody against MuCD41 was used, some platelets were not labeled with gold particles on the surface (data not shown). These observations indicate that NIP-004 administration in mice receiving xenotransplants resulted in the production of human platelets that were morphologically indistinguishable from normal human platelets.

We next studied whether the circulating human platelets in NOG mice were functional. Platelets were obtained from either NIP-004– or vehicle-treated mice. When platelets were stimulated with 10 μM ADP, surface expression of P selectin (CD62p) was observed on human platelets from NIP-004–treated mice at almost

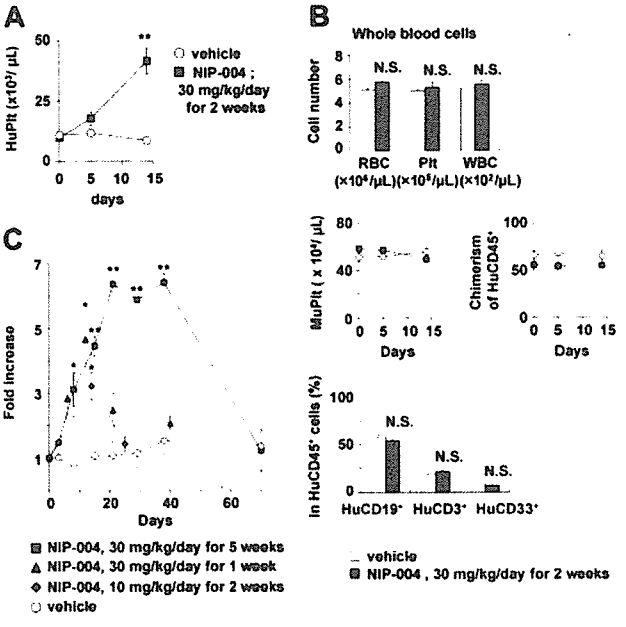

Figure 6. NIP-004–induced production of human platelets in NOG mice receiving xenotransplants. (A) NIP-004 increased the number of circulating human platelets in NOG mice. (B) NIP-004 did not change the number of murine platelets or chimerism of HuCD45$^+$ cells. NIP 004 had no effect on the percentage of human B (CD19$^+$) cells, human T (CD3$^+$) cells, and human myeloid (CD33$^+$) cells in the peripheral HuCD45$^+$ cells. Data from panels A B are expressed as the mean ± SEM (n = 3). (C) NIP-004 increased the number of circulating human platelets. The increase was calculated as the number of circulating human platelets at individual time points divided by the pretreatment value (day 0). Data are expressed as the mean ± SEM (n = 3 to 6) or mean ± SD (n = 2). $^*P < .05$, $^{**}P < .01$ between NIP-004 and vehicle at individual time points. N.S. indicates no significant differences compared with vehicle.

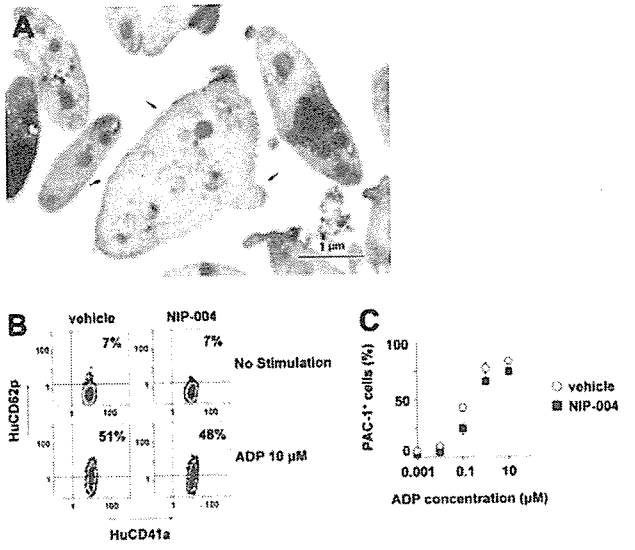

Figure 7. Morphologic and functional features of human platelets induced by NIP-004 in NOG mice. (A) Immunoelectron microscopy using antibody against HuCD41a identified human platelets in PRP derived from NIP-004–treated mice. The surface of a platelet located in the center is labeled with gold particles (arrow), indicating that it is of human origin. Bar, 1 μm. (B) P selectin (HuCD62p) expression upon ADP stimulation in human platelets was similarly increased in both vehicle- and NIP-004–treated mice. (C) After stimulation with various concentrations of ADP, there was a similar dose-dependent escalation in the percentage of PAC-1–positive human platelets from vehicle- and NIP-004–treated NOG mice receiving xenotransplants. PAC-1 antibody specifically recognizes the activated form of GPIIbIIIa. Data are expressed as the mean ± SEM (n = 4).

the same rate as vehicle-treated mice (Figure 7B), suggesting that α-granules were released.[14] In addition, we examined whether the human platelets found in NIP-004–treated mice receiving xenotransplants exhibited a similar response to ADP stimulation as normal platelets (Figure 7C). The active form of fibrinogen receptor (GPIIb-IIIa integrin) on human platelets was recognized by binding of the PAC-1 monoclonal antibody (Figure 7C).[14] Human platelet activation by ADP was dose dependent, and the mean concentration of ADP required to produce 50% activation of the human platelets was 0.6 μM in NIP-004–treated and 0.3 μM in vehicle-treated mice (Figure 7C). These observations indicated that NIP-004 had no adverse effects on the function of human platelets.

Discussion

In this study, we identified a nonpeptidyl synthetic compound, NIP-004, as a novel c-Mpl activator. In vitro studies revealed that rhTPO and NIP-004 display a similar potential to activate HuMpl. However, unlike rhTPO, NIP-004 displays species specificity. Recently, nonpeptidyl small molecule compounds such as benzodiazepine derivatives,[22] hydrazinonaphthalenes and azonaphthalenes,[23,24] and substituted thiazole[25] and xanthocillins[26] have been reported as possessing TPO-like activity. In some cases, c-Mpl agonists such as SB394725 exhibit species specificity.[27] This study confirms that His in the transmembrane domain of c-Mpl is essential for NIP-004 agonist activity (Figure 4B). Although His exists in the transmembrane domain of HuGCSFR and mouse IL-3/GMCSF/IL-5 common β subunit 2 (Muβc2) (ENSP00000342623 and ENSMUSP00000006263 from the Ensembl database, respectively), Ba/F3-HuGCSFR cells expressing Muβc2 and HuGCSFR did not respond to NIP-004 (Figure 1C). Because the position of His in the transmembrane domains of HuGCSFR and Muβc2 does not correspond to HuMpl, we speculate that the His may need to be present in the middle of a transmembrane domain and/or interact with other amino acids of c-Mpl for NIP-004 agonist activity. It has been reported that the point mutation of Leu499 to His in the transmembrane domain of cynomolgus monkey c-Mpl results in the appearance of Mpl agonist activity for SKF-57626, which also possesses HuMpl agonistic activity and does not cause any reactions with cynomolgus monkey c-Mpl,[28] supporting the role of a His residue in the c-Mpl transmembraine domain. Onishi et al previously demonstrated that the point mutation of Ser505 to Asn in the HuMpl transmembrane domain creates a constitutively active form of the receptor,[29] and patients with familial essential thrombocythemia have recently been shown to possess this mutation.[30] Furthermore, mutating Val449 to Gln in the transmembrane domain constitutively activates Huβc.[31] We speculate that mutation in the transmembraine domain of the cytokine receptors may change their conformation and sensitivity to ligand binding or autophosphorylation. Although EPO receptor and growth hormone receptor have been reported to exist in a dimeric form prior to ligand binding,[32,33] no such evidence exists for c-Mpl. Because we have not yet confirmed whether NIP-004 binds directly to HuMpl, further investigation is needed to elucidate its exact mechanisms.

Analysis of human megakaryopoiesis and thrombopoiesis in vivo has been limited to xenotransplantation models, because continual, reproducible reconstruction of human platelet production is difficult using NOD/severe combined immunodeficiency (SCID) or NOD/SCID/β_2m^{null} mice. Perez et al demonstrated that human megakaryopoiesis and thrombopoiesis appeared 1 month after transplantation, and human platelets in these mice were functional using PB-derived $CD34^+$-transplanted NOD/SCID mice.[34] Human platelets were hardly detected in NOD/SCID mice receiving transplants of human CB cells.[34,35] Reconstitution of human megakaryopoiesis was also limited in NOD/SCID/β_2m^{null} mice.[36] We detected human platelets in all animals for 6 months after transplantation with CB-derived $CD34^+$ cells into NOG mice. We therefore believe that the NOG mouse is a suitable animal model for the analysis of human megakaryopoiesis and thrombopoiesis. TPO and c-Mpl are important molecules for megakaryopoiesis and thrombopoiesis. Administration of TPO can induce polyploid megakaryocytes in BM and increase the number of circulating platelets in mice and patients. In contrast, administration of TPO to NOD/SCID mice receiving xenotransplants with human hematopoietic progenitor cells does not alter the number of human platelets.[35] The present study demonstrated that NIP-004 increases the number of human platelets in NOG mice by significantly stimulating human megakaryopoiesis. To the best of our knowledge, this is the first report to demonstrate alteration of human megakaryopoiesis and thrombopoiesis in an animal model of xenotransplantation through c-Mpl activation. In our preliminary data, another TPO mimetic, SB-497115, which has been demonstrated to increase the number of platelets in healthy volunteers,[10] increased the number of circulating $HuCD41a^+$ platelets in NOG mice receiving xenotransplants (data not shown). In conclusion, we demonstrate that NIP-004 acts as a HuMpl activator to enhance CFU-MK formation in vitro and platelet production in vivo. Our new experimental animal model of human megakaryopoiesis may be a useful tool to study megakaryopoiesis in vivo.

Acknowledgments

We thank Dr Kenneth Kaushansky for his critical review; K. Miyaji for chemical construction of the compound; Y. Hirai for construction of HuGCSFR; and A. Ikejima for her technical assistance.

References

1. de Sauvage FJ, Hass PE, Spencer SD, et al. Stimulation of megakaryocytopoiesis and thrombopoiesis by the c-Mpl ligand. Nature 1994;369:533-538.
2. Lok S, Kaushansky K, Holly RD, et al. Cloning and expression of murine thrombopoietin cDNA and stimulation of platelet production in vivo. Nature. 1994;369:565-568.
3. Kaushansky K, Lok S, Holly RD, et al. Promotion of megakaryocyte progenitor expansion and differentiation by the c-Mpl ligand thrombopoietin. Nature. 1994;369:568-571.
4. Wendling F, Maraskovsky E, Debili N, et al. cMpl ligand is a humoral regulator of megakaryocytopoiesis. Nature. 1994;369:571-574.
5. Bartley TD, Bogenberger J, Hunt P, et al. Identification and cloning of a megakaryocyte growth and development factor that is a ligand for the cytokine receptor Mpl. Cell. 1994;77:1117-1124.
6. Kaushansky K, Drachman JG. The molecular and cellular biology of thrombopoietin: the primary regulator of platelet production. Oncogene. 2002; 21:3359-3367.
7. Kuter DJ, Begley CG. Recombinant human thrombopoietin: basic biology and evaluation of clinical studies. Blood. 2002;100:3457-3469.
8. Li J, Yang C, Xia Y, et al. Thrombocytopenia caused by the development of antibodies to thrombopoietin. Blood. 2001;98:3241-3248.
9. Ito M, Hiramatsu H, Kobayashi K, et al. NOD/SCID/gamma(c)(null) mouse: an excellent recipient mouse model for engraftment of human cells Blood. 2002;100:3175-3182.
10. Jenkins J, Nicholl R, Williams D, et al. An oral, non-petide, small molecule thrombopoietin receptor agonist increases platelet counts in healthy subjects [abstract]. Blood. 2004;104:797a. Abstract 2916.
11. Jackson CW. Cholinesterase as a possible marker for early cells of the megakaryocytic series. Blood. 1973;42:413-421
12. Matsumoto A, Masuhara M, Mitsui K, et al. CIS, a cytokine inducible SH2 protein, is a target of the JAK-STAT5 pathway and modulates STAT5 activation. Blood. 1997;89:3148-3154.
13. Suzuki H, Yamazaki H, Tanoue K. Immunocytochemical studies on co-localization of alpha-granule membrane alphaIIbbeta3 integrin and intragranular fibrinogen of human platelets and their cell-surface expression during the thrombin-induced release reaction. J Electron Microsc (Tokyo). 2003;52:183-195.
14. Hagberg IA, Lyberg T. Blood platelet activation evaluated by flow cytometry: optimised methods for clinical studies. Platelets. 2000;11:137-150.
15. Guideline for animal experimentation [in japanese]. Exp Anim. 1987;36:285-288.
16. Komatsu N, Kunitama M, Yamada M, et al. Establishment and characterization of the thrombopoietin-dependent megakaryocytic cell line, UT-7/TPO. Blood. 1996;87:4552-4560.
17. Komatsu N, Nakauchi H, Miwa A, et al. Establishment and characterization of a human leukemic cell line with megakaryocytic features: dependency on granulocyte-macrophage colony-stimulating factor, interleukin 3, or erythropoietin for growth and survival. Cancer Res. 1991;51: 341-348.
18. Takatoku M, Kametaka M, Shimizu R, Miura Y, Komatsu N. Identification of functional domains of the human thrombopoietin receptor required for growth and differentiation of megakaryocytic cells. J Biol Chem. 1997;272:7259-7263
19. Komatsu N, Yamamoto M, Fujita H, et al. Establishment and characterization of an erythropoietin-dependent subline, UT-7/Epo, derived from human leukemia cell line, UT-7. Blood. 1993;82: 456-464.
20. Vainchenker W, Deschamps JF, Bastin JM, et al. Two monoclonal antiplatelet antibodies as markers of human megakaryocyte maturation: immunofluorescent staining and platelet peroxidase detection in megakaryocyte colonies and in in vivo cells from normal and leukemic patients. Blood. 1982;59:514-521.
21. van den Oudenrijn S, von dem Borne AE, de Haas M. Differences in megakaryocyte expansion potential between CD34(+) stem cells derived from cord blood, peripheral blood, and bone marrow from adults and children. Exp Hematol. 2000; 28:1054-1061.
22. Kimura T, Kaburaki H, Tsujino T, Ikeda Y, Kato H, Watanabe Y. A non-peptide compound which can mimic the effect of thrombopoietin via c-Mpl. FEBS Lett. 1998;428:250-254.
23. Duffy KJ, Price AT, Delorme E, et al. Identification of a pharmacophore for thrombopoietic activity of small, non-peptidyl molecules. 2. Rational design of naphtho[1,2-d]imidazole thrombopoietin mimics. J Med Chem. 2002;45:3576-3578.
24. Duffy KJ, Darcy MG, Delorme E, et al. Hydrazinonaphthalene and azonaphthalene thrombopoietin mimics are nonpeptidyl promoters of megakaryocytopoiesis. J Med Chem. 2001;44: 3730-3745.
25. Inagaki K, Oda T, Naka Y, Shinkai H, Komatsu N, Iwamura H. Induction of megakaryocytopoiesis and thrombocytopoiesis by JTZ-132, a novel small molecule with thrombopoietin mimetic activities. Blood. 2004;104:58-64.
26. Sakai R, Nakamura T, Nishino T, et al. Xanthocillins as thrombopoietin mimetic small molecules Bioorg Med Chem. 2005;13:6388-6393.
27. Erickson-Miller CL, DeLorme E, Tian SS, et al Discovery and characterization of a selective, nonpeptidyl thrombopoietin receptor agonist. Exp Hematol. 2005;33:85-93.
28. Erickson-Miller CL, Delorme E, Iskander M, et al. Species specificity and receptor domain interaction of a small molecule TPO receptor agonist [abstract]. Blood. 2004;104:795a.
29. Onishi M, Mui AL, Morikawa Y, et al. Identification of an oncogenic form of the thrombopoietin receptor MPL using retrovirus-mediated gene transfer. Blood. 1996;88:1399-1406.
30. Ding J, Komatsu H, Wakita A, et al. Familial essential thrombocythemia associated with a dominant-positive activating mutation of the c-MPL gene, which encodes for the receptor for thrombopoietin. Blood. 2004;103:4198-4200.
31. Jenkins BJ, D'Andrea R, Gonda TJ. Activating point mutations in the common beta subunit of the human GM-CSF, IL-3 and IL-5 receptors suggest the involvement of beta subunit dimerization and cell type-specific molecules in signalling. EMBO J. 1995;14:4276-4287.
32. Constantinescu SN, Keren T, Socolovsky M, Nam H, Henis YI, Lodish HF. Ligand-independent oligomerization of cell-surface erythropoietin receptor is mediated by the transmembrane domain. Proc Natl Acad Sci U S A. 2001;98:4379-4384.
33. Brown RJ, Adams JJ, Pelekanos RA, et al. Model for growth hormone receptor activation based on subunit rotation within a receptor dimer. Nat Struct Mol Biol. 2005;12:814-821.
34. Perez LE, Rinder HM, Wang C, Tracey JB, Maun N, Krause DS. Xenotransplantation of immunodeficient mice with mobilized human blood CD34(+) cells provides an in vivo model for human megakaryocytopoiesis and platelet production. Blood. 2001;97:1635-1643.
35. Perez LE, Alpdogan O, Shieh JH, et al. Increased plasma levels of stromal-derived factor-1 (SDF-1/CXCL12) enhance human thrombopoiesis and mobilize human colony-forming cells (CFC) in NOD/SCID mice. Exp Hematol. 2004;32:300-307.
36. Angelopoulou MK, Rinder H, Wang C, Burtness B, Cooper DL, Krause DS. A preclinical xenotransplantation animal model to assess human hematopoietic stem cell engraftment. Transfusion. 2004;44:555-566.

ELSEVIER

EXPERIMENTAL HEMATOLOGY

Experimental Hematology 34 (2006) 1239–1247

Development of human–human hybridoma from anti-Her-2 peptide–producing B cells in immunized NOG mouse

Yoshie Kametani[a,f], Masashi Shiina[a], Ikumi Katano[a], Ryoji Ito[a], Kiyoshi Ando[b], Kanae Toyama[a], Hideo Tsukamoto[c], Takuya Matsumura[a], Yuki Saito[d], Dai Ishikawa[g], Takao Taki[g], Mamoru Ito[h], Kohzoh Imai[i], Yutaka Tokuda[d], Shunichi Kato[e], Norikazu Tamaoki[h], and Sonoko Habu[a,f]

[a]*Department of Immunology;* [b]*Department of Hematology and Oncology;* [c]*Laboratory for Molecular Science Research;* [d]*Department of Surgery;* [e]*Department of Pediatrics;* [f]*Center for Embryogenesis and Organogenesis, Tokai University School of Medicine, Kanagawa, Japan;* [g]*Molecular Medical Science Institute, Otsuka Pharmaceutical Co. Ltd., Tokushima, Japan;* [h]*Central Institute for Experimental Animals, Kanagawa, Japan;* [i]*First Department of Internal Medicine, Sapporo Medical University, Hokkaido, Japan*

(Received 3 December 2005; revised 24 April 2006; accepted 4 May 2006)

Objective. **Numerous monoclonal antibodies have been developed for the purpose of medical treatments, including cancer treatment. For clinical application, the most useful are human-derived antibodies. In this study, we tried to prepare designed antigen-specific antibodies of completely human origin using immunodeficient mouse.**

Methods. **Nonobese diabetic/severe combined immunodeficient/IL-2 receptor γ null mouse (NOG) mouse was used to reconstitute the human immune system with umbilical cord blood hematopoietic stem cells (CB-NOG mouse) and to prepare human-derived Her-2-epitope–specific antibodies. Hybridoma lines were prepared by fusing the human myeloma cell line Karpas707H.**

Results. **Serum of immunized NOG mouse contained human-derived immunoglobulin M (IgM) antibodies specific for a short peptide sequence of 20 amino acids, including the epitope peptide of apoptotic Her-2 antibody CH401. Hybridoma lines were successfully prepared with spleen B cells obtained from the immunized CB-NOG mouse. One of these cell lines produced human IgM against the epitope peptide that can recognize surface Her-2 molecule.**

Conclusion. **We could produce human-derived IgM antibody against Her-2 epitope peptide in CB-NOG mouse, succeeding in generation of human hybridoma-secreting IgM against a given peptide.** **© 2006 International Society for Experimental Hematology. Published by Elsevier Inc.**

Passive monoclonal antibody (mAb) therapy has been accepted as a treatment for cancers and autoimmune diseases for the past decade [1,2]. For patients affected by cancer, passive mAb therapy is of benefit mainly because the immune reaction of most patients is suppressive. To date, several antibodies such as Trastuzumab (Herceptin) and Rituximab have been already under practical use, and some are under clinical investigation. Therapeutic effectiveness of these antibodies, to some extent, promotes development of new monoclonal antibodies related to the disease [3]. In addition to cancer patients, anti-tumor necrosis factor-α mAb of human–mouse chimera mAb (Infliximab), or of completely humanized mAb (Adalimumab) are used for suppression of T-cell function in rheumatoid arthritis and Crohn's disease, and are proved to be relatively successful [4,5].

In consideration of clinical application, therapeutic antibody is ideal to be humanized. Today, almost all antibodies for clinical use are derived from mouse, at least in part, although they were humanized by techniques of molecular biology [6]. Recently, the mouse line carrying human chromosome fragments containing immunoglobulin (Ig) gene cluster was developed, which made it possible to prepare completely human-type antibodies produced by mouse B cells [7]. However, these mice produce IgG with sugar chains of mouse origin. Although sugar chains are

Offprint requests to: Sonoko Habu, M.D., Ph.D., Department of Immunology, Tokai University School of Medicine, Boseidai, Isehara, Kanagawa, 259-1193 Japan; E-mail: sonoko@is.icc.u-tokai.ac.jp

0301-472X/06 $–see front matter.
doi: 10.1016/j.exphem.2006.05.006

thought to have low immunoreactivity induced by species-specificity, the risk to induce human anti-mouse antibody production remains [8]. Therefore, the most ideal system is that of antibodies of human origin produced by human B cells.

We have developed a human immune system reconstituted in the mouse environment by transplanting human hematopoietic stem cells in immunodeficient mouse [9,10]. In comparison with nonobese diabetic-severe combined immunodeficient (NOD-SCID) mice, NOD-SCID–IL-2Rγ knockout mouse (NOG) showed higher engraftment of human hematopoietic cells and higher proportion of T-cell development in the xenogenetic environment [11]. In a previous study, we reconstituted the human immune system in NOG mouse with umbilical cord blood hematopoietic stem cells (CB-NOG) and found that immunization of 2,4-dinitrophenol-conjugated keyhole limpet hemocyanin (DNP-KLH) induces antigen-specific human IgM production [12]. These findings indicate that the reconstituted human immune system has developed potential for producing antibodies against the immunized antigens, although the net number of human T and B cells per head in CB-NOG mice is less than one tenth that in normal mouse.

To obtain human-derived antibody to effectively suppress tumor cells or mass, we can immunize CB-NOG mice with a particular epitope, which is recognized by an apoptotic antibody. Among the reported monoclonal antibodies against Her-2 established by mouse and the epitopes reported [13–16], some possessed suppressive effect for tumor growth. Ishida and collaborators [17] established a humanized monoclonal antibody termed CH401, which has an epitope different from Herceptin and induces apoptosis to Her-2–expressing cells efficiently. In this article, we focus on the capacity of human B cells developed in mouse environment to produce antigen-specific antibodies, to analyze if CH401-recognizing epitope can induce human B cells to produce epitope-specific antibody in CB-NOG mouse. As a result, we determined that the CB-NOG mouse produced specific antibodies against a short peptide of 20 amino acids carrying the CH401 epitope. Consequently, the antibody-producing B cells were fused with a human myeloma cell line, Karpas707H [18], to establish a hybridoma line.

Materials and methods

Mice

NOD/Shi-scid, common γc-null (NOD/SCID/γc-null; NOG) mice were provided from the Central Institute for Experimental Animals (Kawasaki, Japan). BALB/c mice were purchased from Crea Japan Inc. (Kawasaki, Japan). All mice were kept under specific pathogen-free conditions in the animal faculty located at the Tokai University School of Medicine (Isehara, Japan).

Human hematopoietic stem cells

Human umbilical cord blood was obtained from full-term healthy newborns immediately after vaginal delivery. Informed consents were obtained according to Institute guidelines, and this work was approved by Tokai University Human Research Committee. Mononuclear cells (MNCs) were separated by Ficoll-Paque gradient centrifugation. $CD34^+$ cells were purified from MNCs using the two-step MACS system (Miltenyi Biotec, Gladbach, Germany). The purity was >98%.

Transplantation

Nine-week-old NOG mice were irradiated sublethally with 2.5 Gy prior to transplantation, and $CD34^+$ cells were transplanted intravenously. Eight weeks after transplantation, peripheral blood was collected via orbit under inhalation anesthesia. MNCs were prepared and reconstitution efficiencies were calculated by hCD45 expression analyzed by fluorescein-activated cell sorting (FACS) analysis.

Peptides

Her-2 peptide includes the sequence identified as the epitope of an apoptotic anti-Her-2 antibody, CH401, which was determined using multiple antigen peptides (MAP) peptides with a partial amino acid sequence of Her-2 (Miyako et al., manuscript in preparation). The sequence of the peptide is N:163-182 ((YQDTILWK-DIFHKNNQLALT-BBB)8-K4K2KB). This peptide was synthesized using Rink amide resin (0.4–0.7 mmol/g) and peptide synthesizer ACT357 (Advanced Chemtech, Louisville, KY, USA). On the 96-well plate, each of these MAP peptides was coated and the cross-reactivity with CH401 was examined by enzyme-linked immunosorbent assay (ELISA).

Monoclonal antibodies, flow cytometry, and cell sorting

All cells were analyzed using FACS Calibur (Becton Dickinson, Franklin Lakes, NJ, USA). For each analysis or sorting, living gate white blood cells or lymphocytes were further gated on human $CD45^+$ cells. Mouse anti-human mAbs included peridinine chlorophyll protein-conjugated CD45, T-cell receptor (TCR), CD1a, fluorescein isothiocyanate (FITC)-conjugated CD4, IgM, phycoerythrin-conjugated CD4, CD8, IgD, and allophycocyanin (APC)-conjugated CD19.

Immunization, EBV transformation, and hybridoma preparation

Eight to 10 weeks after transplantation, mice were immunized intraperitoneally with 2,4-dinitrophenylated keyhole limpet haemocyanin (DNP-KLH; 100 μg/alum/head), toxic shock syndrome toxin-1 (TSST-1; 25 μg/alum/head), Her-2 extracellular domain (25 μg/alum/head) or Her-2 epitope peptide (100 μg/FCA/head). Mice were immunized every 2 weeks. Four days after the last booster, mice were sacrificed and spleen cells were collected. Epstein-Barr virus (EBV) transformation was performed by conventional method. Four weeks after EBV treatment, culture supernatants were collected and specific-antibody–producing clones were selected by ELISA, as described previously [9]. The cells secreting specific antibodies were expanded and fused with a human myeloma cell line, Karpas707H, using polyethylene glycol. Hybridomas were selected by Ouabine and HAT. Positive clones were selected by ELISA.